POLITECNICO DI TORINO

Corso di Laurea Magistrale
In ingegneria dei materialli

Numerical Simulation of the Thermo-Mechanical Behaviour in Tread-Braked Railway Wheels

PROFESSOR:
Prof. Niccolò Zampieri
Prof. Matteo Magelli

STUDENT :
Mersedeh Rahimi

Academic year

2025/2026

ACKNOWLEDGMENTS

I want to thank everyone who has been with me on this journey sincerely, First, I want to appreciate my great supervisors ,**professor Nicolò Zampieri and Dr. Matteo Magellei**, for their helpful advice, support and guidance throughout this project. Thank you very much for your perfect knowledge and information you have shared with me during this time.

I also appreciate Politechnico di Torino as a great university for giving us this precious opportunity to demonstrate our talents and to develop our education. This trust and support opened the new door to our future life, and I am profoundly grateful for opportunity to gain experience, learn, grow, and challenge myself in this environment.

To my beloved family thank you for everything. Also, to my incredible friends, thank you for filling this journey with joy, motivation, and unforgettable moments. Your friendship meant a lot to me; those words can express. This thesis is not just a reflection of my academic efforts, it reflects the love, support, and inspiration I received from all of you. Thank you for being part of my story.

.

ABSTRACT

The tread-braked system is used in freight trains because it is simple, reliable, and cost-effective. However, during braking, the frictional contact between the brake block and the wheel generates a significant amount of heat. Over time, this heat can alter the wheel surface, causing wear, crack initiation, and finally degrading the material properties of the wheel. For this reason, it is essential to understand how thermal loads influence the wheel by using the finite element method.

In this study, the thermal behavior of tread-braked wheels will be discussed in detail by ANSYS Workbench. This thermal simulation includes two different cases: one that is two-dimensional and another that is three-dimensional. The two-dimensional model is used for showing the temperature distribution across the whole wheel. On the other hand, the three-dimensional models allow us to see how heat affects the wheel in a more detailed way, especially when the simulation includes a brake block. By using these models, we can better understand what happens to the wheel in steady-state conditions during braking. Apart from that, time has been considered a parameter and determines the thermal behavior of the wheel under a transient state.

The simulations were carried out using data adapted from studies based on real experimental investigations performed on a 1:5 scaled twin-disc tribometer. This experimental framework follows Pascal's similitude theory and incorporates a novel thermal scaling approach proposed by Zampieri and Magelli. Particular attention was devoted to evaluating the influence of heat-flux application, contact geometry, mesh refinement, and time scaling on the predicted temperature field. The results prove that the 3D model, including the brake block, is capable of capturing localized temperature gradients and higher peak temperatures, which are not fully represented in the simplified axisymmetric models.

The obtained results are used as guidance to choose the suitable materials for the wheel and brake block and design a better braking system. Studies like this make reliable mechanical design, better maintenance strategies, and enhanced safety in railway operations.

Contents

List of figures:

List of tables:

1 Introduction

The braking system is one of the most critical components for maintaining the safety, reliability, and operational efficiency of trains. During braking, a large amount of kinetic energy is generated. This energy must be dissipated to keep acceptable stop distances and protect the mechanical components of the system. Among the different braking technologies developed for railway applications, tread braking systems are widely used in freight trains.

Although modern passenger trains increasingly rely on disc brakes because of their higher efficiency and reduced maintenance requirements, the tread braking systems are used continuously in freight transportation. Due to the simple design, easy maintenance, and affordability, they are ideal for heavy-duty and long-distance operations. The generated heat between the brake block and the tread part directly influences the durability of the wheel and leads to several important phenomena, such as thermal expansion, microstructural changes, and material degradation [1].

For these reasons, the study of tread-braking systems is an important topic for academic research and industrial applications. Understanding the thermo-mechanical processes during braking provides useful information to make more efficient wheels and brake blocks, as well as better insights for predictive models capable of representing real operating conditions. All these can make freight railway transportation safer, more sustainable, and more economically efficient. [2]

1.1 Goals and aims of the activity:

The main objective of this thesis is to analyze the thermo-mechanical behavior of tread-braked railway wheels during braking conditions. The study is based on numerical modeling approaches that can predict the temperature distribution in the wheel during braking, with particular attention to the localized heated parts at the wheel–block contact interface. To achieve this objective, both two-dimensional (2D) axisymmetric and three-dimensional (3D) finite element models are developed and analyzed under steady-state and transient thermal conditions. The 2D model provides an efficient thermal response for the wheel, while the 3D models allow a more detailed investigation of the localized heated area and the influence of the contact geometry between the brake block and the wheel.

Another important goal of this work is to evaluate the influence of several modeling parameters, including heat-flux application, mesh refinement, time stepping, and thermal scaling, on the predicted temperature field. Particular attention is devoted to the comparison between simplified numerical models and more realistic configurations that include the brake block. [2]

Finally, the results of the study discuss wear mechanisms and material performance, showing the importance of accurate thermal modeling for better material selection and improving the durability and reliability of railway braking systems.

1.2 Thermal Behavior of Tread Braking Systems

The thermal behavior of the tread braking system is studied by using two complementary approaches: numerical simulation and experimental analysis. Each approach provides unique and valuable information. Numerical models allow an accurate and adjustable study of operating conditions, material properties, and design parameters within a wide range, thus enabling the investigation of scenarios that are difficult, expensive, or unsafe to reproduce experimentally. [1] In particular, finite element models are considered effective tools to predict temperature fields and the thermomechanical behavior of railway wheels under braking.

On the other hand, experimental tests enable the direct observation of physical phenomena occurring during braking and can be a privileged means of validation in numerical predictions. For this reason, experimental methods are a crucial step in the assessment of heat generation, thermal contact conditions, and material behavior under realistic operating conditions. Therefore, the combination of both approaches can be used as a full assessment of the thermal mechanisms in tread braking and facilitates the development of accurate predictive models. [2][3]

1.3 Numerical Methods

Numerical methods are the base part in the analysis of thermal simulation during braking. Over the years, several computational ways have been developed to model frictional heat generation and the resulting temperature evolution at the wheel–block interface. Early approaches often relied on finite difference methods due to their simplicity and efficiency in solving one-dimensional or axisymmetric heat conduction problems. Significant progress in this field was achieved by the development of finite element models, especially on tread-braked railway wheels.

In the article “Simulation of the thermo-mechanical behavior of tread-braked railway wheels by means of a 2D finite element model," Bosso, Magelli, and Zampieri proposed a two-dimensional axisymmetric model that can simulate the thermo-mechanical behavior of wheels under braking conditions. This model has outstanding efficiency in computation and the accurate capture of the temperature evolution in the wheel. [1]

Further developments were introduced by the same authors in “A novel finite element axisymmetric model with non-axisymmetric thermal loads for thermal analyses of tread-braked wheels,” where a novel axisymmetric formulation including non-axisymmetric thermal loads was presented. This approach improved the localized heated parts with great computational efficiency. In addition, the research presented in "Adapting a scaled twin-disc device for tread braking investigations based on an ad-hoc thermal similitude model” described a 1:5 scaled twin-disc device and a thermal similitude framework to ensure consistency between laboratory testing and full-scale braking conditions. This scaling methodology allows the controlled reproduction of thermo-mechanical phenomena while preserving the fundamental physical mechanisms in heat generation and dissipation. [4][5]

Today, the finite element method is the most widely used numerical tool for simulating tread-brake systems. It provides detailed discretization of the wheel and brake block geometry, customized boundary conditions, and transient heat flux distributions. Moreover, it allows the evaluation of thermo-mechanical effects on the wheel, such as thermal stresses, deformation, and crack initiation during real braking operation. [2]

Furthermore, numerical modeling offers perfect flexibility in difficult, costly, or unsafe operating conditions, such as severe braking or long-term cyclic loading. For these reasons, numerical approaches are now considered essential tools for the design of safer, more efficient railway braking systems.

1.4 Experimental Methods

Experimental methods are necessary to validate numerical predictions and attain a comprehensive understanding of the function of the physical phenomena. Over the years, several different experimental methods have been created. These include full-scale and scaled laboratory test benches that are designed to simulate braking conditions in a controlled environment. The best way to see how brakes work is to test them on real condition. [2]

Full-scale simulation of real braking conditions using actual wheel–block assemblies, allowing controlled variation of braking force, speed, and contact pressure. In parallel, scaled experimental devices, such as twin-disc tribometers, reproduce the essential thermal and mechanical mechanisms of tread braking while reducing cost and improving experimental flexibility.

Full-scale experiments usually are costly and time-consuming and are often limited in terms of the parameters that can be controlled and the ability to repeat them. To overcome these limitations,

laboratory-based test benches have been widely considered in the research and development laboratory.[2][3]

Typically, laboratory benches consist of a rotating wheel or wheel segment driven at a prescribed angular velocity. A brake block is pressed against the wheel under a controlled normal force, thereby simulating a braking event, as shown in fig. 1-1.[6][7] Temperature evolution is monitored by using thermocouples, infrared sensors, and, in some cases, high-speed thermal cameras. These instruments allow us to measure the transient temperature, identify hot spots, evaluate the heat partition ratio between wheel and block to observe surface transformations such as oxidation, crack initiation, and material transfer.

These kinds of experiments can be done under various braking scenarios, including single braking events, repeated cycles, or emergency braking conditions. This flexibility makes it possible to analyze key parameters, such as braking force, initial speed, sliding distance, environmental temperature, heat dissipation, and material degradation. In addition, modern experimental test benches often incorporate ventilation systems or controlled airflow devices due to convection heat and to reproduce realistic cooling conditions. The airflow control improves the laboratory experiments and enhances the correlation between laboratory results and on-field measurements.[4]

Experimental observations contribute to clarifying the development of thermal gradients, hot spots, crack initiation, and surface degradation processes that occur under repeated braking cycles. The next section provides a brief description of test bench available at the Railway Laboratory of Politecnico di Torino.

1.5 Test Bench for Tread Braking Experiments

This equipment is defined as one of the experimental tools and practical methods used to simulate tread braking under controlled laboratory conditions. Instead of testing full-scale components, the device adopts a reduced configuration that allows accurate control of key operating parameters such as normal load, sliding speed, and braking duration. This method allows us to separate the main factors that affect heat generation while still keeping a strong physical resemblance to real braking situations, as shown in the experimental methods described in the literature [4]. The bench is designed to reproduce both steady-state and transient braking phases.

In this equipment, a rotating disc or wheel-like specimen represents the wheel tread, while a stationary counter-body simulates the action of the brake block. During operation, frictional contact between these two components generates heat, which is partially dissipated through the wheel specimen and partially through the brake block. This method enables us to simulate temperature distribution and peak temperatures at the contact interface, which has a critical role in wheel damage, thermal fatigue, and material degradation.

The performance of the test bench is developed by an advanced instrumentation system, which allows us to monitor the temperature evolution on the contact surface. The data acquisition system provides high temporal resolution, allowing it to capture rapid thermal transients during braking events.

This test bench represents a reliable and flexible experimental method. Its capability to reproduce realistic thermal loads under controlled conditions makes it particularly suitable for supporting numerical studies of railway wheel behavior during braking.

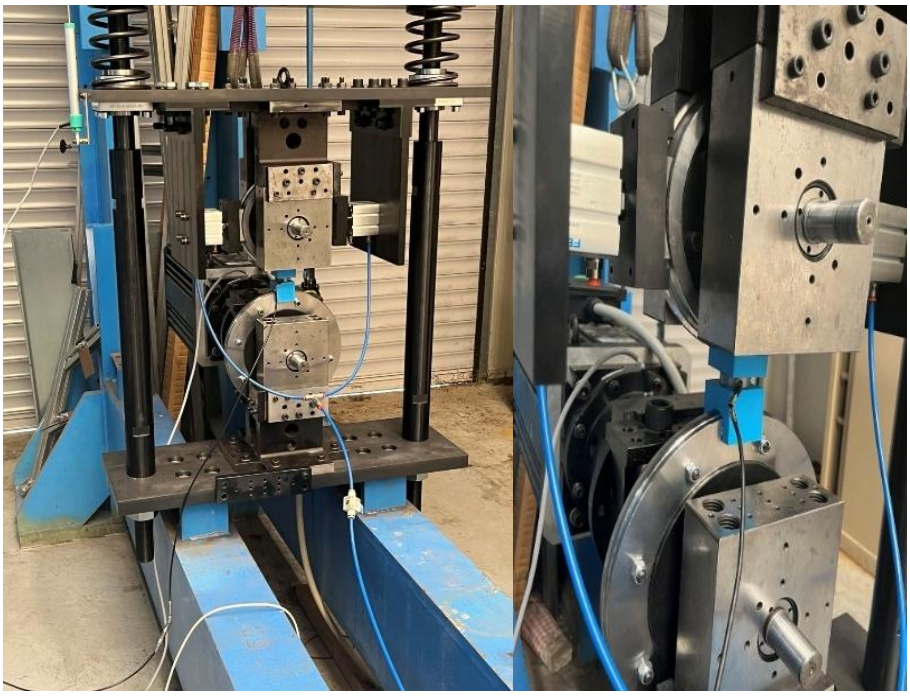

Figure 1-1: Twin desk test bench in railway laboratory of Politecnico di Torino.

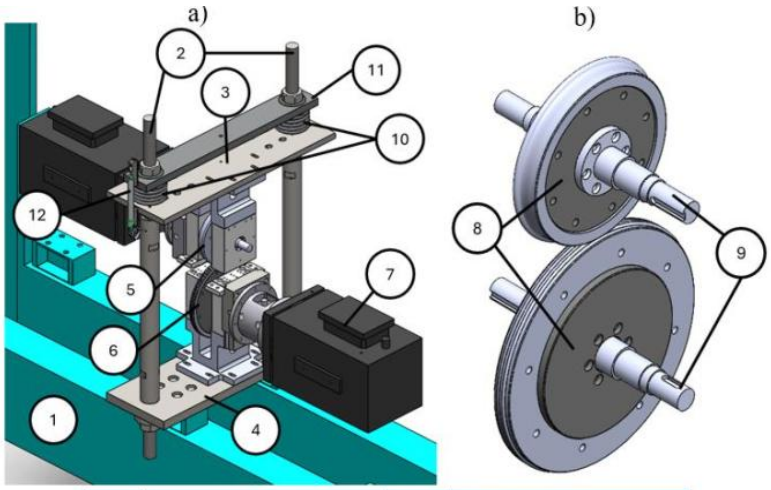

No.	Label	No.	Label
1	Rigid frame	7	Brushless motor
2	Traction rods	8	Disc hubs
3	Upper plate	9	Disc shafts
4	Lower plate	10	Helical springs
5	Wheel disc	11	Loading beam
6	Rail disc	12	Linear potentiometer

Figure 1-2: Overview of the twin disc tribometer design.[4]

1.6 Method Comparison in Thermal Analysis

Numerical and experimental methods together provide a perfect reference to analyze tread-braking systems. Experimental methods provide physical realism and reliable data about the actual wheel and block behavior under load. In turn, numerical simulations can extend these findings to a wider range of operating conditions, geometries, and material combinations that would be difficult or impractical to assess experimentally. Combining the two aspects creates a deeper understanding of the thermal behavior in tread brakes, leading to better design and more sustainable braking systems for freight railways.

The thermal behavior of a railway wheel is analyzed in this study under steady-state and transient operating conditions, and the temperature fields obtained from two- and three-dimensional analyses are compared. The numerical framework is based on the finite element method (FEM), with particular emphasis on the discretization process to catch the thermal response accurately. Special attention is devoted to the representation of the temperature distribution in different regions of the wheel for better understanding of the mechanisms responsible for uneven wear, thermal gradients, and material degradation during braking.

1.7 Structure of the Thesis

The present study is organized in five chapters; these contents are briefly summarized as below:

Chapter 2 introduces a two-dimensional model of the wheel and presents an analysis under axisymmetric steady-state thermal conditions. This investigation provides an overview of the temperature distribution in the wheel and indicates the hot spots that may lead to surface degradation and uneven wear.

Chapter 3 describes in detail the three-dimensional numerical model and analyzes the thermal behavior of the wheel under steady-state conditions. In addition, this chapter investigates the effect of including the brake block, which introduces a localized thermal load on the tread surface. The simulations allow the evaluation of frictional heat generation during braking and its influence on the thermal field and performance of the wheel–brake system.

Chapter 4 presents and compares the results obtained from the different dimensional configurations. This analysis shows the influence of braking on temperature distribution, thermal concentrations, and wear development and also offers comprehensive knowledge about the thermo-mechanical behavior of rail wheels during braking. A mesh convergence experiment is provided in this chapter to confirm the accuracy of the numerical model. In addition to steady-state conditions, the transient thermal response is investigated on both 2D and 3D models to obtain the time dependence of heat generation and temperature evolution during braking.

Chapter 5 focuses on material selection and possible future developments based on the numerical results obtained in this work. Particular attention is given to the suitable materials that improve thermal efficiency, reduce surface damage, and extend the service life of both the wheel and the brake block. The chapter concludes with a discussion of design improvements for better performance and sustainability in railway braking systems.

2 Thermal 2D Simulation of Tread-Braked Wheels With FEM

2.1 Axisymmetric (2D) Thermal Model

This simulation was started by importing the CAD format of the wheel that extended from the hub to the region of the tread. This two-dimensional model is considered to analyze the thermal behavior of the railway wheel and uses geometric symmetry. As shown in fig. 2-1, the model is a single radial cross-section; this simplification is possible because the heat flux during braking is assumed to be uniformly distributed along the wheel. As a result, the computational effort is mainly reduced while keeping a prominent level of accuracy in the predicted thermal response. [1]

Several works emphasized that 2D models show the thermal behavior of tread-braked wheels accurately, Vernersson's studies on modeling and calibration of wheel temperatures, as well as recent 2D finite-element analysis by Bosco, Zampieri, and Magellei, demonstrate that axisymmetric formulations can predict the temperature distribution and heat-transfer mechanisms with excellent agreement to experimental measurements. [2][3]

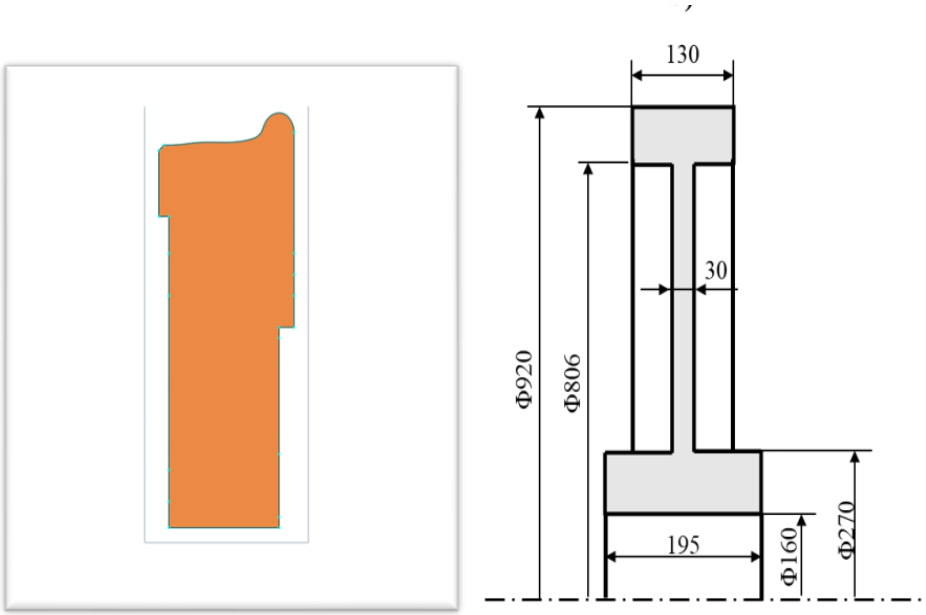

Figure 2-1:Radial cross section of the rail wheel and Simplified wheel section geometry (dimensions in mm)[5].

2.1.1 Geometry Transformation and Rotation

According to ANSYS workbench analysis, the global X-axis shows the radial direction, and the global Y-axis related to wheel axis. Due to this issue, a rotated coordinate system was defined to correct any geometric misalignment. The wheel cross-section was transformed and rotated 90 degrees to align these axes with the model geometry, this indicates that the heat flux and boundary conditions are applied in the true direction of the tread surface, rather than in a global axis direction.

This is critical issue to ensure that temperature gradients and heat flow are correctly interpreted in post-processing. It also means that the applied loads are fully consistent with the true profile of the wheel, which in turn enhances numerical accuracy and reliability in the simulation.

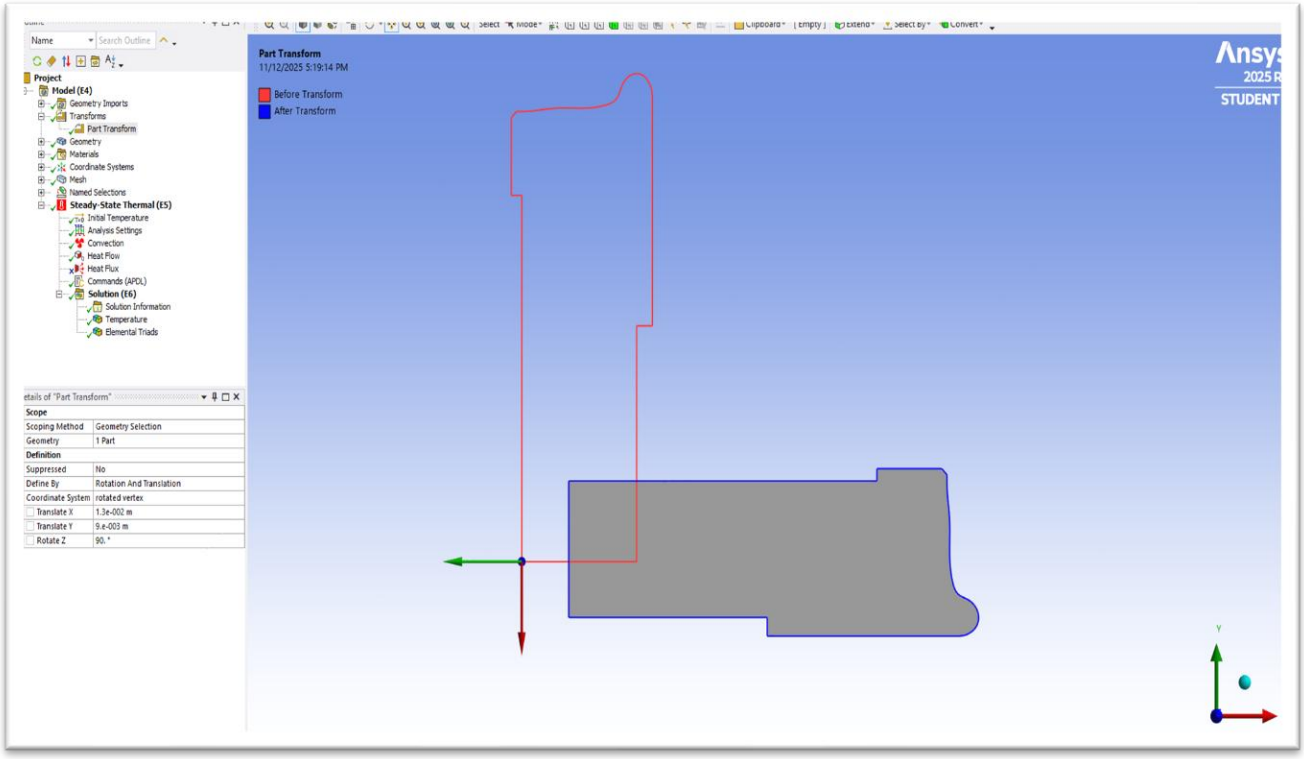

Figure 2-2: Transformation and rotation of the geometry by 90°.

2.1.2 Geometry and Scaling Consideration

The input data used to define the thermal boundary conditions were obtained from scaled tests rather than full-scale, and it is important to ensure consistency between the laboratory measurements and the numerical model. The geometric scale factor $\varphi_L = 5$, which is considered in this simulation, is based on experimental configuration developed by Zampieri, Magelli, and co-authors in their studies on tread-braked wheels and scaled tribometers. [4]

The selection of $\varphi_L = 5$ is not an arbitrary quantity but reflects the experimental setup adopted in the research. This scale factor provides safe and economic testing conditions while keeping the physical mechanisms, such as frictional heat generation and dissipation during braking. Once the geometric scale factor is defined, the other physical quantities are scaled according to the adopted similitude framework. The comparison of the classical Pascal scaling approach with the proposed thermal scaling rule is indicated in Table 2-1.

Quantity	Pascal Scaling Rule	Novel Scaling Rule
Length	(φ_L)	(φ_L)
Area	(φ_L^2)	(φ_L^2)
Time	(φ_L)	(φ_L^2)
Speed	1	(1^*)
Force	(φ_L^2)	(φ_L)
Weight	(φ_L^3)	(φ_L^3)
Heat flux	1	(φ_L^{-1})
Thermal energy	(φ_L^3)	(φ_L^3)
Convection coefficient	Not addressed	(φ_L^{-1})
Temperature	Not addressed	1

Table 2-1: Comparison between Pascal scaling factors and the novel similitude scaling factors[4].

2.1.3 Material Definition and Mesh Refinement Strategy

The wheel material was considered structural steel, which is used in railway applications due to its high strength, toughness, and excellent thermal conductivity at high temperatures. The thermal properties of structural steel are assumed as fig2-3. that the density is 7850 kg/m³, specific heat capacity is 434 J/kg°C, and thermal conductivity is 60.5 W/m°C.

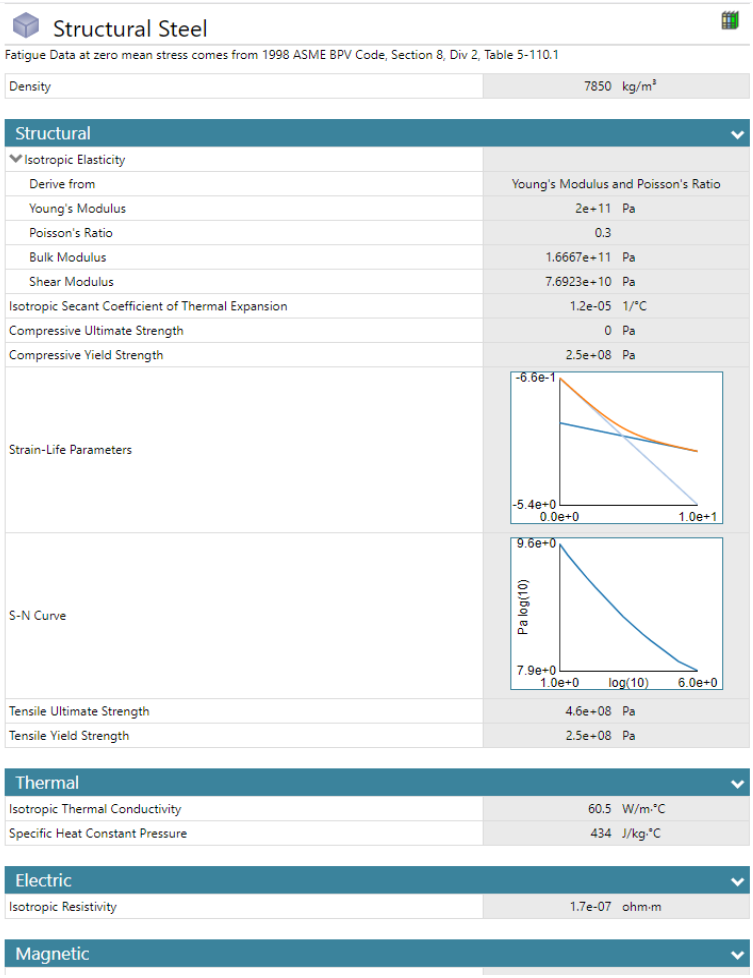

Figure 2-3: Material properties of steel structural.

The finite element mesh was created by quadrilateral elements for axisymmetric thermal analysis. The mesh element was selected as 0.002 m with a good balance between accuracy and computational efficiency. Furthermore, local mesh refinement and edge sizing controls were introduced on the tread surface where the heat flux was applied. This ensured that steep temperature gradients and heat transfer within the wheel rim and tread interface could be captured more precisely. The refined mesh provided smoother temperature contours and more stable numerical convergence, which justified the fact that the chosen discretization was adequate for both steady-state simulations.

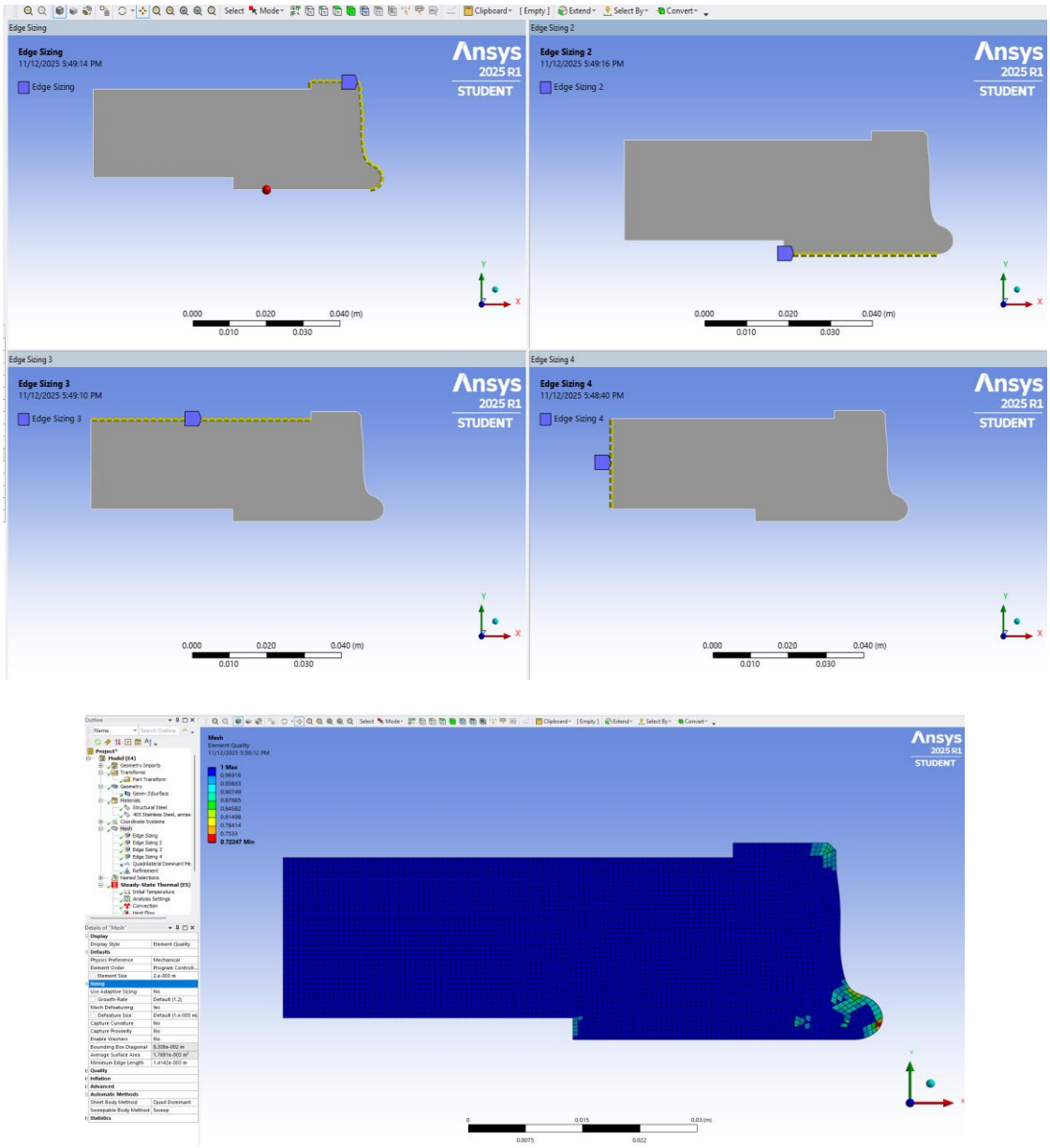

Figure 2-4: Mesh refinement and edge sizing in the 2D geometry.

In the axisymmetric (2D) model, the thermal behavior is assumed to be uniform along the entire wheel. To obtain physically realistic results, a heat-partitioning approach is adopted to account for the fraction of braking energy absorbed into wheel. In the present study, the heat partition factor was considered equal to ($\beta = 81.9\%$). [3]

The heat partition factor depends on the thermal properties of the materials in contact. In better words, it is controlled by their thermal effusivity, defined as equation 2-1:

$$e = \sqrt{\lambda \rho c}, \qquad (2\text{-}1)$$

where λ is the thermal conductivity, ρ the density, and c the specific heat capacity. Since the steel wheel has higher thermal effusivity than the cast-iron brake block, a larger fraction of the generated frictional heat is transferred into the wheel. A detailed comparison of the selected materials and their influence on the thermal response will be presented in chapter 5, following the discussion of the future development of the simulation.

The tread region was identified as the outer surface in the model with a named selection as the red edge that is indicated in fig. 2-5. This selection defines the exact portion of the wheel geometry where the thermal load is applied.

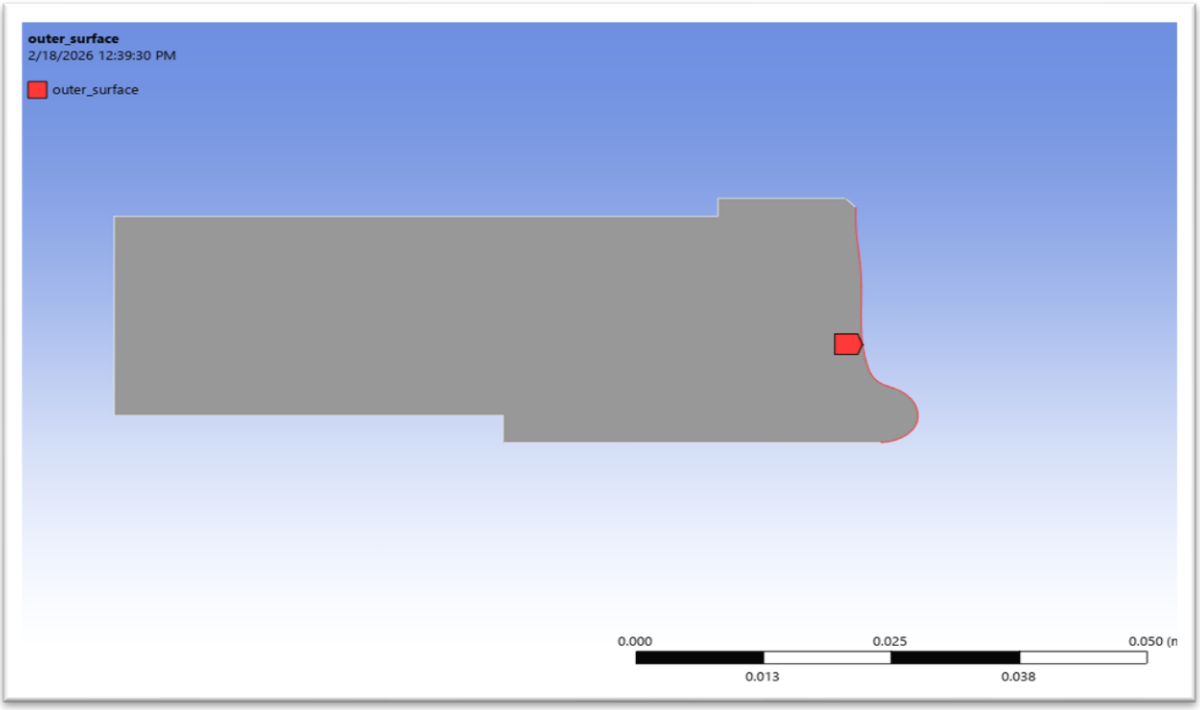

Figure 2-5: Defined edge part in named selection as outer surface .

Due to the wheel geometry, tread width is 80 mm in the full-scale model, whereas, in the scaled model, with a scaling factor of 1:5, the tread width will be 16 mm. So, the thermal load applied on the tread region from −6 mm to +10 mm in the transverse direction, the scaled effective heated zone in the model, is shown in fig. 2-7.

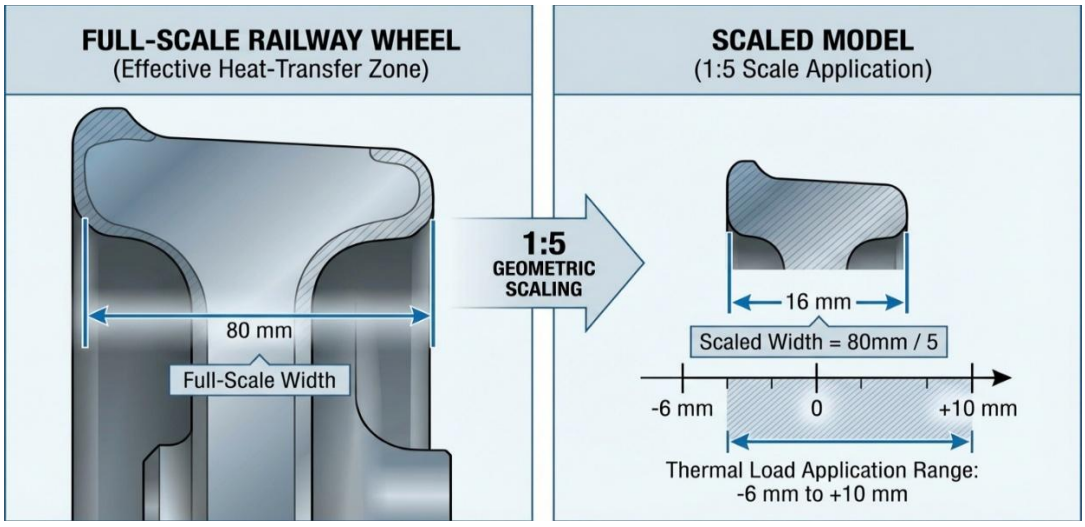

Figure 2-6: Tread named selection in scaled 2D geometry.

Thermal model analysis was done by using an APDL command, as shown in fig. 2-6. This modeling approach ensures consistency between the physical braking scenario and the numerical implementation, both in terms of the location and magnitude of the applied thermal load.

Commands

```
!   Commands inserted into this file will be executed just prior to the ANSYS SOLVE command.
!   These commands may supersede command settings set by Workbench.

!   Active UNIT system in Workbench when this object was created:  Metric (m, kg, N, s, V, A)
!   NOTE:  Any data that requires units (such as mass) is assumed to be in the consistent solver unit system.
!                See Solving Units in the help system for more information.


PREP7

heat_flux = 8e5

!CSLIST
llist

/solu

cslist
csys,12
cmsel,s,outer_surface,node
nlist
nsel,r,loc,y,-6e-3,10e-3
nlist
ESLN
ELIST

csys,0
!sf,all,hflux,heat_flux
sfe,all,2,hflux,,heat_flux
allsel
```

Figure 2-7: APDL comment for 2D thermal simulation in steady state.

To calculate the average frictional heat flux at wheel-shoe contact, equation 2-2 is used for full-scale heat flux (2Bg configuration) [4]:

$$(\Phi_{ws})_f = \frac{Q_{ax}}{2 \cdot N_B} \cdot g \cdot i_s \cdot V \cdot \frac{1}{L_s H_s} \qquad (2\text{-}2)$$

Where:

- Q_{ax}= axle load
- N_B= number of brake shoes per wheel, (N_BFor 2Bg configuration= 2)
- g= gravity
- i_s= slope
- V= speed
- L_s= shoe circumferential length, tread length=Ls=130mm=0.13m
- H_s= shoe axial width, tread width, Hs=80mm=0.08m

Reference case for drag braking condition (TSI Wag) used for the simulation[4]:

- Axle load $Q_{ax} = 22.5$tons
- Speed $V = 70$km/h
- Slope $i_s = 21‰ = 0.021$

"For the considered operating scenario, the total heat flux generated by friction at each wheel-shoe contact is 880,170 W/m² on the full-scale system."

$$(\Phi_{ws})_f = 880170 \text{ W/m}^2$$

Partitioning for cast iron (2Bg) is specified as 0.819 [4]:

$$\Phi_w = \Phi_{ws} \cdot \beta \qquad (2\text{-}3)$$

$$\Phi_w = 880170 \times 0.819$$
$$\Phi_w \approx 720849 \text{ W/m}^2$$

So, for 2Bg cast iron configuration, the correct full-scale heat flux to the wheel is:

$$\boxed{720\,849 \text{ W/m}^2}$$

In tread braking, the full-scale wheel–block contact generates 880,170 W/m² as a total frictional heat flux, as shown in equation 2-2. After applying the partitioning factor and the novel scaling proposed by Zampieri and Magelli, heat flux is achieved by equation 2-3. In this simulation, the amount of heat flux imposed on the tread region is considered 8×10^5 W/m² approximately. All the wheel surfaces, except the tread, were subjected to convection with a heat-transfer coefficient of 300 W/m²°C and supposed ambient air at 22°C.

As expected, the tread region exhibits extremely high temperatures. In particular, the middle part of the tread shows the highest thermal concentration since this part is in direct contact with the wheel and experiences more frictional heat. The resulting temperature field is shown in fig2-8 and highlights the differences across the various regions of the wheel.

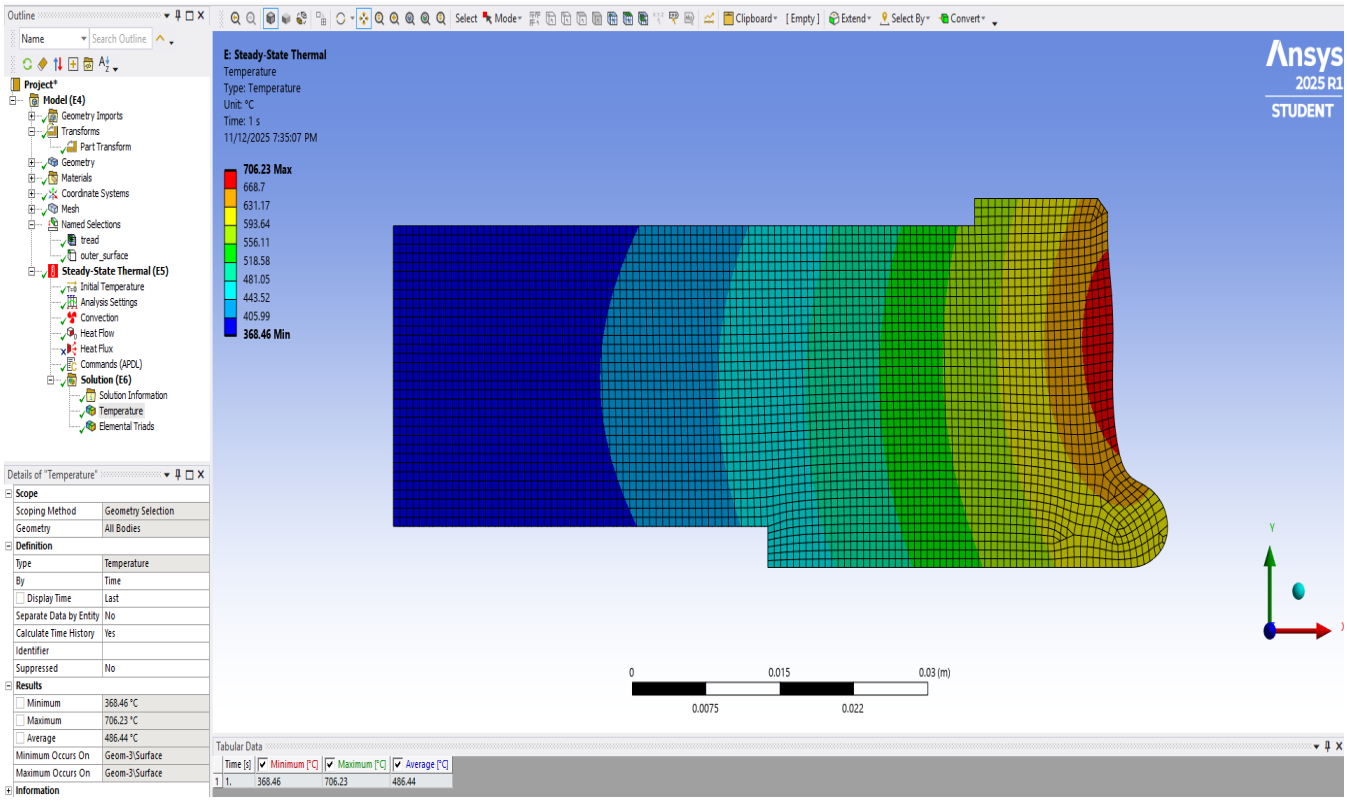

Figure 2-8: Result of steady state axisymmetric simulation in 2D geometry of rail wheel.

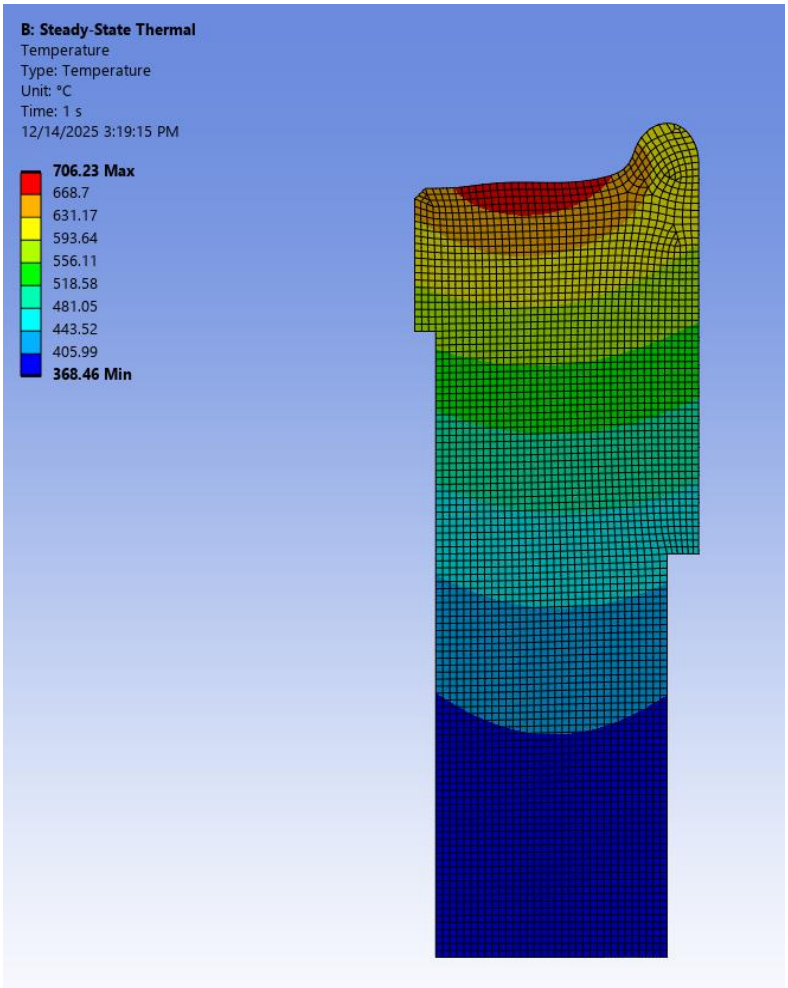

Figure 2-8: Result of steady state axisymmetric simulation in 2D geometry of rail wheel.

Temperature Result (steady-state)	Minimum(℃)	Maximum(℃)	Average (℃)
	368.46	706.23	486.44

Table 2-2: Result of steady state axisymmetric simulation in 2D geometry of rail wheel.

3 Thermal 3D Simulation of Tread-Braked Wheels With FEM

3.1 Three-Dimensional (3D) Thermal Model

In addition to the two-dimensional analysis, a three-dimensional (3D) thermal model was developed in a steady-state condition. The 2D axisymmetric models are not suitable for detecting local temperature peaks that may cause microstructural changes in the wheel, and they cannot model the temperature field in the circumferential direction. The 3D model serves as a numerical check of the axisymmetric thermal solution and evaluates possible effects under similar loading conditions. This model will be discussed in two parts. First, the thermal behavior of the wheel is discussed under simplified and controlled axisymmetric conditions. Then, we will examine the localized effects of the wheel, including the brake block.[1][5]

3.1.1 3D steady state Model without Brake Blocks

The 3D wheel model in ANSYS was generated by the same geometry used in the 2D model. Heating conditions and geometry are perfectly symmetric; the applied heat flux and convection boundaries were kept identical to those used in the 2D model.

The model is discretized by using a quadrilateral mesh with the same element size used before, which is refined by edge sizing to ensure higher accuracy in the tread region, where the highest temperature gradients occur. Then the 2D cross-section model was revolved 360° around the wheel's central axis (x) by using the "Pull" function in the edit mesh to generate the 3D solid mesh. The model was divided into 120 layers to ensure smooth continuity of elements along the circumferential direction and keep a consistent thermal distribution throughout the geometry, as shown in Fig. 3-1.

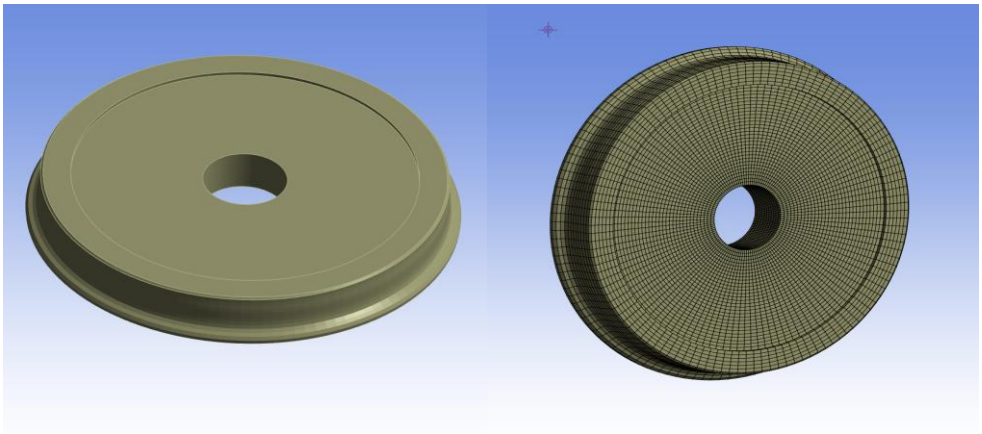

Figure 3-1: Geometry of the 3D model after generation.

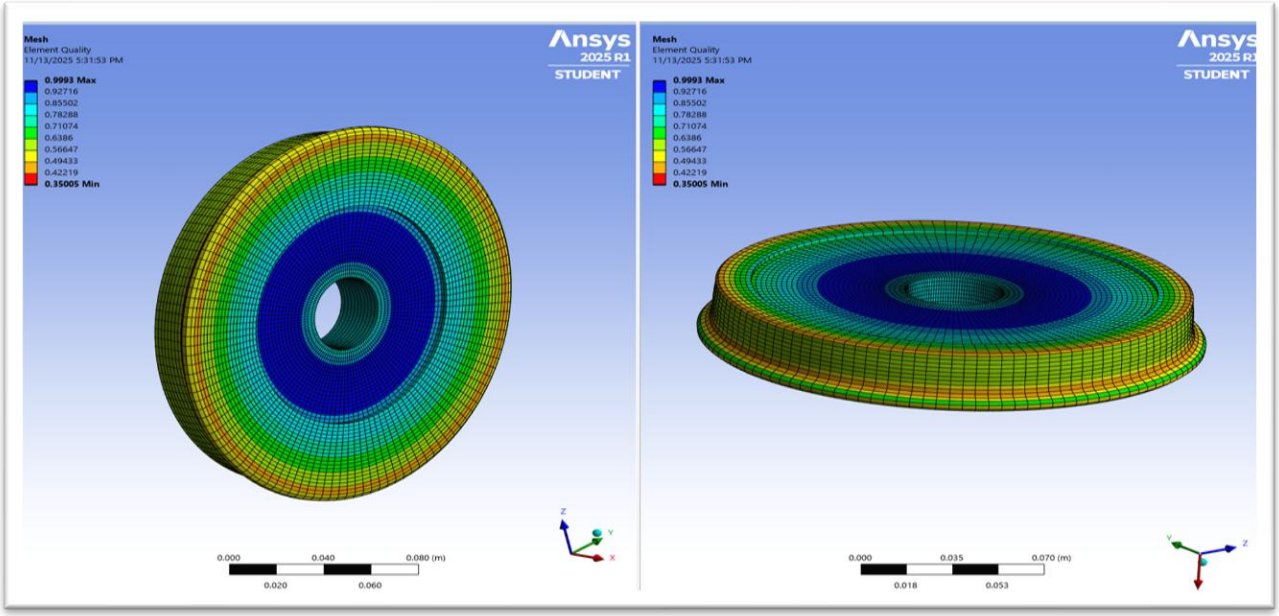

Figure 3-2: Element quality and mesh refinement in 3D geometry.

3.1.2 Named Selection of the Tread Region

In the 3D model, a named selection was defined to identify the exact tread surface of the wheel where the heat flux is applied. This region represents the geometrical contact area between the brake block and the wheel during tread braking. The external radius of the scaled wheel was considered 92 mm. In addition, a radial zone extending from −6 mm to 10 mm was selected as an area where the heat flux is applied, which is provided in table 3-1. The portion of frictional heat transferred to the wheel is then determined by the heat partition factor, which is considered (β = 81.9%) for the cast iron brake block which reflects the influence of the different thermal properties of the two different contacting bodies.[4]

Action	Entity type	Orientation	Operator	Unit	Value	Lower band	Upper band	Coordinate system
Add	Element face	Location z	Range	m	NA	-0.006	0.01	Coordinate sys1
Filter	Element face	Location x	Greater than or equal	m	0.092	-	-	Coordinate sys1

Table 3-1: Tread named selection due to partition factor in 3D geometry

Figure.3-3 indicates the tread region in the 3D axisymmetric model and clarifies the tread geometrical configuration.

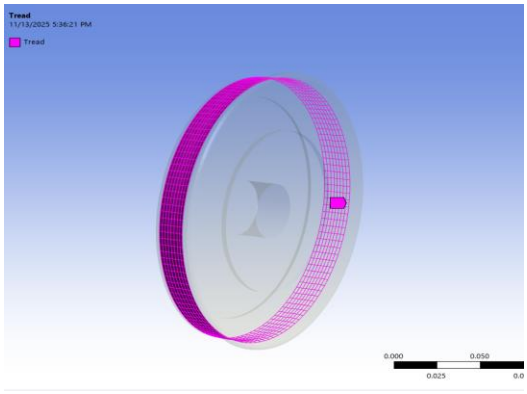

Figure 3-3: Tread named selection in 3D geometry.

the same material properties and boundary conditions in the 2D model were applied in the 3D simulation; convective heat transfer was applied to all external steel wheel surfaces, with a heat flux of 8×10^5 W/m², a heat transfer coefficient of 300 W/m²·°C, and an ambient temperature of 22°C.
Figure3-4 shows the 3D model with boundary conditions.

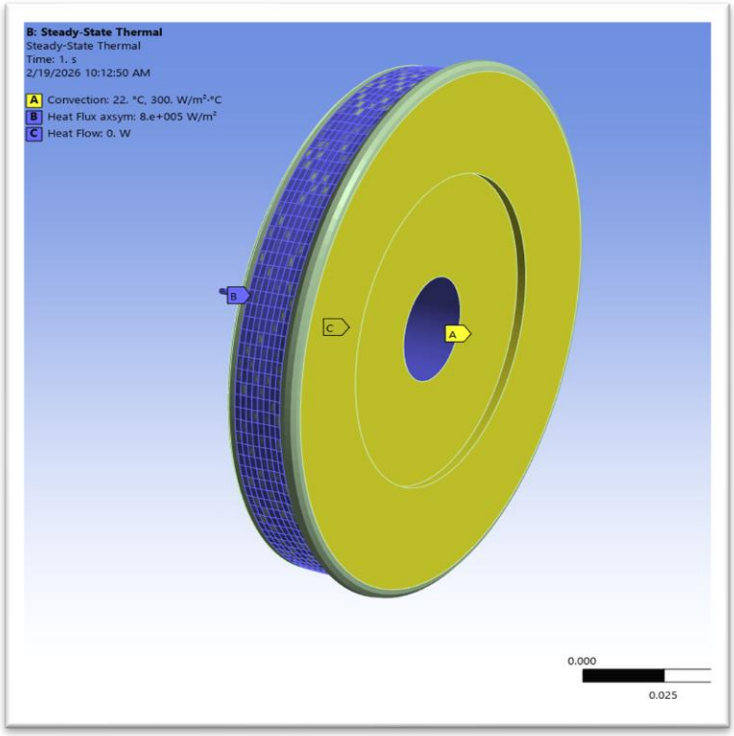

Figure 3-4: Infographic of 3D model with boundary condition.

Then the simulation was done, and the results displayed a smooth temperature gradient from the tread region (where the heat flux was applied) toward the inner parts. The maximum temperature was measured at the tread surface, reaching about 706°C, confirming that this zone undergoes the highest thermal load during braking. The temperature decreased slowly in the radial direction, reaching 368°C near the hub, due to thermal dissipation by conduction and convection. Steady-state results showed the 3D axisymmetric model reproduces the same thermal behavior as those obtained from the 2D analysis and has high numerical consistency. The steady-state model provides a reliable reference to assess the long-term thermal equilibrium of the wheel during continuous braking.

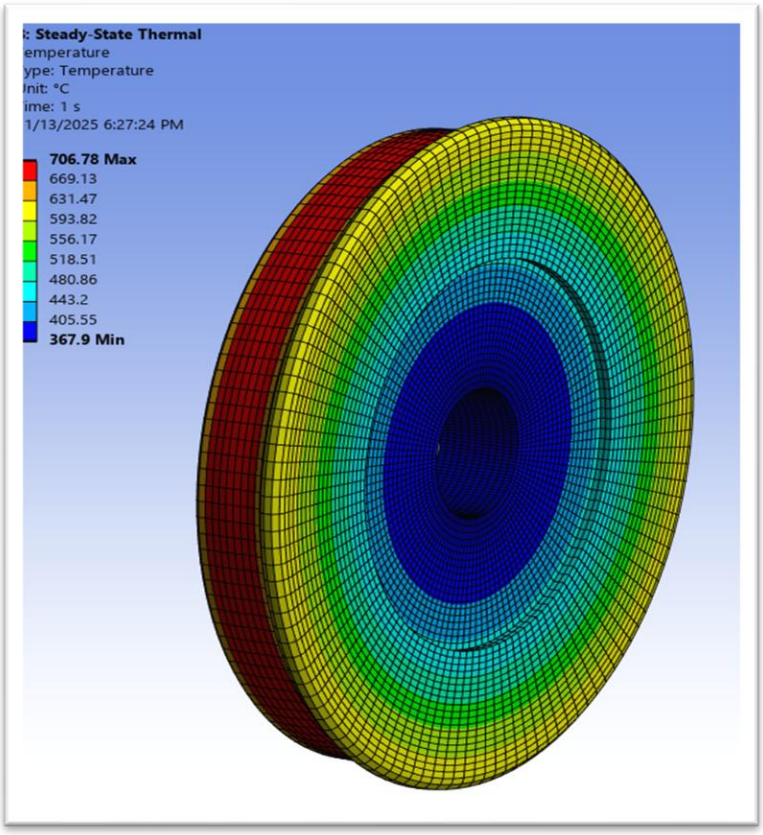

Figure 3-5: Result of steady state axisymmetric simulation in 3D geometry of rail wheel.

Temperature Result (steady-state)	Minimum(℃)	Maximum(℃)	Average (℃)
	397.9	706.78	486.44

Table 3-2: Result of steady state axisymmetric simulation in 3D geometry of rail wheel.

3.2 3D Model with brake blocks

In this part, the brake blocks were added in the 3D model to replicate the real condition and localized heat generation during braking. This setup enables the study of non-axisymmetric temperature distributions and local variations in heat flux during braking. The model is arranged according to the actual 2Bg/2Bgu configuration (in which two blocks act on opposite sides of the wheel tread). [5] Heat flux is applied on the contact interface to simulate the frictional power input from braking conditions. The most critical step in this model is to correctly define the brake block's position and its contact area on the wheel, considering the exact block–wheel angle, and to apply the scaled heat flux accurately on this specific region.

3.2.1 Brake Block position

The angular position of the brake blocks around the wheel was determined by relating the brake block's arc length to the scaled wheel's radius. Due to the experimental data, the angle of contact area between wheel and brake block is defined by equation (3.1) and indicated in fig.3-6.

- block length : 64 mm.
- full scale external radius of the wheel: 460 mm
- scaled external radius of the wheel : 92 mm,

$$\theta = 64/92 = 0.7 \qquad (3.1)$$

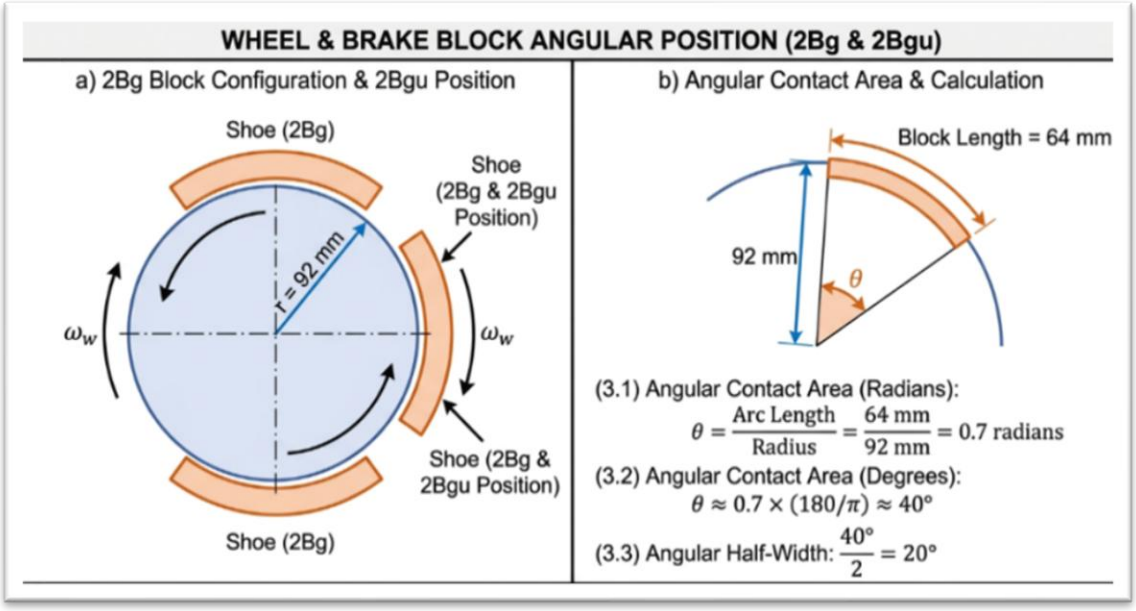

Figure 3-6: Angular contact area between scaled wheel and brake block.

This value represents the fraction of a full circular radian corresponding to the block's contact area. To express this angle in degrees, the value is multiplied by the conversion factor 180/π since the block acts symmetrically around its central contact line, the angular half-width becomes as below:

$$\theta = 0.7 \times 180/\pi \approx 40^\circ \quad , \quad 40^\circ/2 = 20^\circ \tag{3.2}$$

To define the block influence symmetrically, this angle was divided into two equal parts, providing 20° on each side of the central reference direction. Using the vertical axis as the primary reference (90° and 270° for upper and lower positions), the two upper brake blocks are therefore located between 70° and 110°. The two lower ones are placed at symmetric intervals between 250° and 290°; these parts were shown in fig. 3-7. The calculated angular sector defines the effective contact regions of each brake block and is essential for representing their thermal impact in the numerical model.

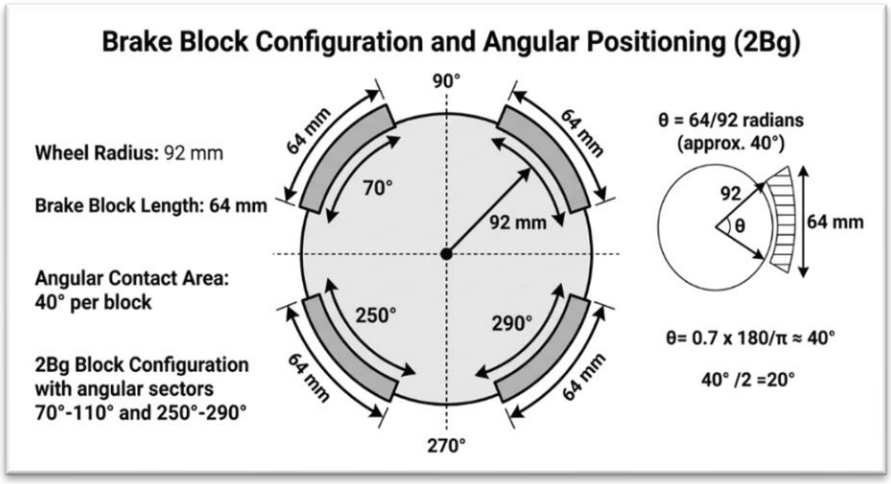

Figure 3-7: 2Bg block configuration by considering angular contact area between wheel and brake block.

Following the scaled methodology proposed in the article "Adapting a scaled twin-disc device for tread braking investigations based on an ad-hoc thermal similitude model," the local heat flux applied to the brake block is scaled. This scaling factor compensates for the reduced geometric contact area in the 1:5 configuration. It ensures that the thermal load remains consistent with the real frictional energy at the block–wheel interface. As shown in equation (3.3), by the inverse of the geometric scale for heat flux, the resulting temperature field remains consistent with the equivalent full-scale braking event.

$$\varphi_L = 1/\varphi_L \tag{3.3}$$

$$\varphi_L = 5 \ , \ \varphi_L^{-1} = 0.2 \tag{3.4}$$

following the obtained scale in equation3-4, the effective heat flux imposed on the block contact region in the 3D model is approximately 36,800 W/m², as shown in equation (3.5).

Heat flux for blocks = Scaled radius wheel * (Heat flux(total) / φ_L^{-1}) (3.5)

- Scaled radius wheel = 0.092 m
- Heat flux(total) = 800,000 W/m²
- Heat flux for blocks=36,800 W/m²

Although all steps remain identical between the 2D and 3D configurations, the definition of the boundaries in 3D, including a block for the tread region, differs due to variations in the contact area. In such cases, different boundary conditions must be introduced to distinguish the different thermal loads acting on the specified surface and obtain accurate temperature distribution. The tread part will be defined due to named selection, as shown in fig. 3-8 and table 3-3. By assigning the corresponding boundary conditions, the model can capture the temperature distribution accurately, ensuring that the heat input is applied only on correct regions of the wheel–block interface.

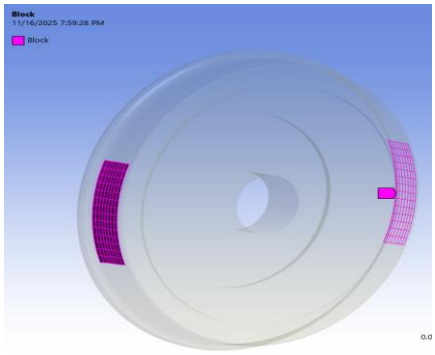

Figure 3-8: Brake block part in wheel contact area.

Action	Entity type	Orientation	Operator	Unit	Value	Lower band	Upper band	Coordinate system
Add	Element face	Location y	Range	deg	-	70	110	Coordinate sys1
Add	Element face	Location y	Range	deg	-	250	290	Coordinate sys1
Filter	Element face	Location x	Greater than or equal	m	0.091	-	-	Coordinate sys1
Filter	Element face	Location z	Range	m	-	-0.006	0.01	Coordinate sys1

Table 3-3: Tread named selection in block wheel contact area.

For the heat convection boundary, additional parameters were defined to represent the heat-transfer conditions on the exposed surfaces, including non-tread and non-brake block parts. These parts were specified based on rail-wheel geometry. Tables 3-4 and 3-5 clearly show these parts.

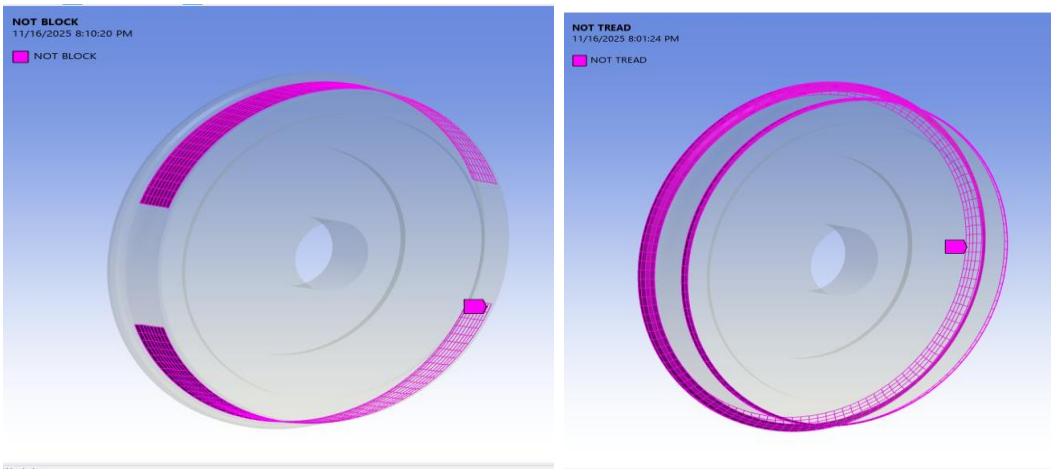

Figure 3-9: Non-tread and non-block part in block wheel contact area.

Action	Entity type	Orientation	Operator	Unit	Value	Coordinate system
Add	Element face	Location z	less than or equal	m	-0.006	Coordinate sys1
Add	Element face	Location z	Greater than or equal	m	0.01	Coordinate sys1
Filter	Element face	Location x	Greater than or equal	m	0.091	Coordinate sys1

Table 3-4: Non-Tread part in block wheel contact area.

Action	Entity type	Orientation	Operator	Unit	Value	Lower band	Upper band	Coordinate system
Add	Element face	Location x	Greater than or equal	m	0.091	-	-	Coordinate sys1
Filter	Element face	Location z	Range	m	-	-0.006	0.01	Coordinate sys1
Remove	Element face	Location y	Range	deg	-	70	110	Coordinate sys1
Remove	Element face	Location y	Range	deg	-	250	290	Coordinate sys1

Table 3-5: Non-block part in block wheel contact area.

The boundary condition and scaling thermal load have been defined correctly, due to the block location in steady state and non-axisymmetric condition which has been shown in fig.3-10.

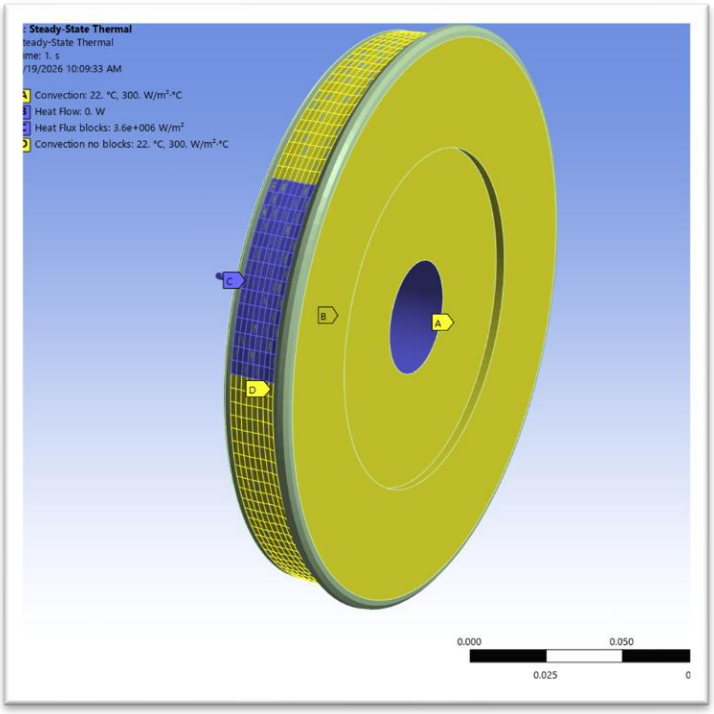

Figure 3-10: Infographic of 3D model including block with boundary condition.

The simulation was run, and the result was obtained as shown in fig. 3-11 and table 3-6. It is evident that including the brake block into the 3D simulation creates a non-axisymmetric condition, which increases the maximum temperature compared to axisymmetric models. This increase is expected since the heat is not distributed uniformly along the tread but instead applied to a small contact area. Because of this localized heating, the model reaches a temperature of 1688°C, reflecting the intense concentration of frictional power in the block contact area.

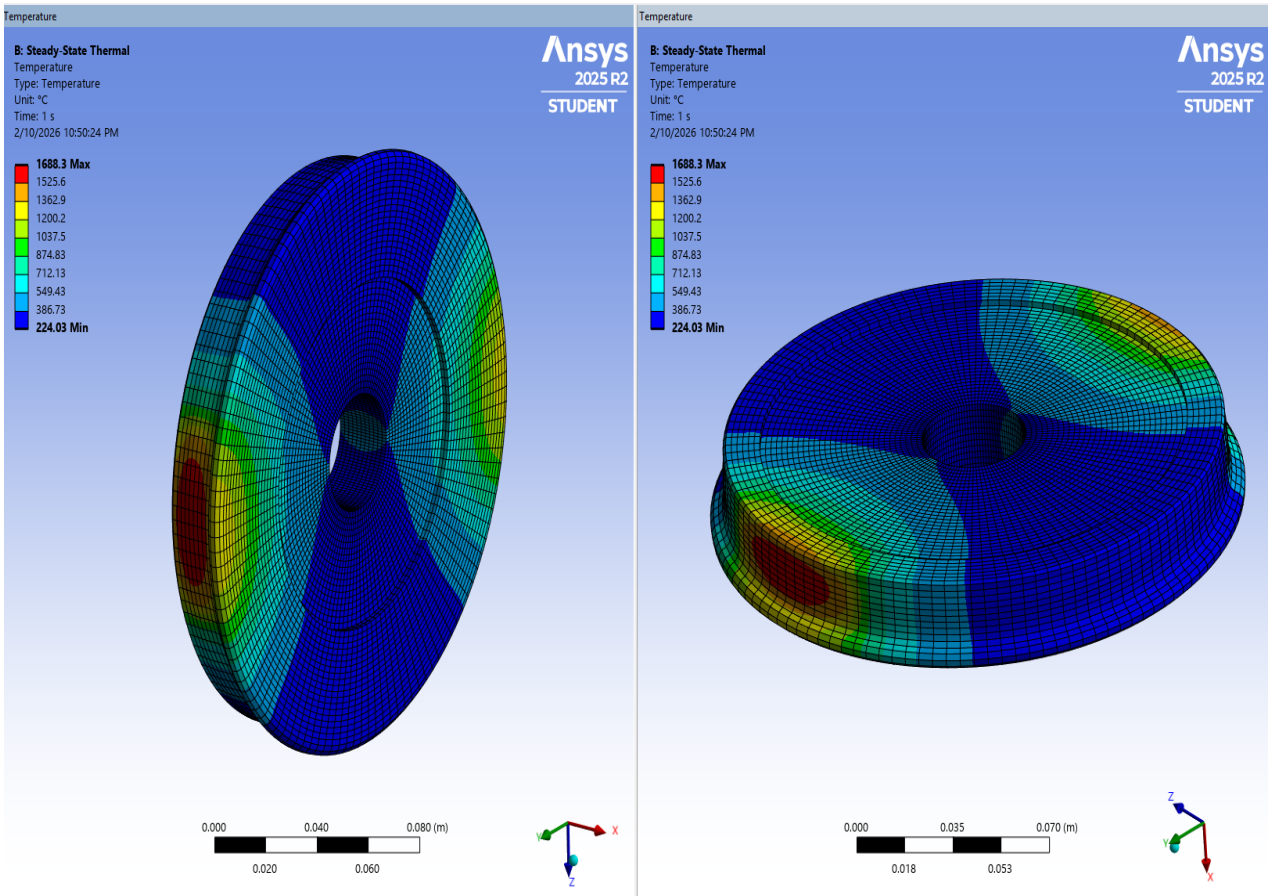

Figure 3-11: Result of block -wheel simulation in 3D geometry of rail wheel.

Temperature Result (steady-state)	Minimum(℃)	Maximum(℃)	Average (℃)
	224.03	1688.3	459.02

Table 3-6: Result of block -wheel simulation in 3D geometry of rail wheel.

4 Result and Analysis

4.1 Steady-State Thermal Analysis

This chapter reports the result of thermal behavior on 2D and 3D finite element models of the rail wheel under tread braking conditions, both in the steady state and transient axisymmetric configuration and in a more realistic case where the brake block is included. The analyses were conducted under identical material properties, thermal loads, and boundary conditions to ensure comparability between modeling approaches. Special attention is given to the influence of mesh refinement, the heat-flux-applied region, and the adopted novel scaling rule on the resulting temperature distribution.

4.1.1 Results of the 2D Axisymmetric Model

The 2D axisymmetric model provides a simple way to study the thermal behavior on the wheel during braking. Instead of the full three-dimensional geometry, a single radial cross-section is considered, which significantly reduces computational cost while still capturing the dominant heat conduction mechanisms. After correcting the heat-flux orientation by transforming the model and refining its mesh to resolve a convergence discrepancy, the thermal load was assigned to the outer tread edge.

As we saw in chapter two, the steady-state simulation predicts a maximum temperature of 706°C at the tread part, with the hottest zone where braking heat enters the wheel. Temperatures decrease rapidly in the radial direction, while axial variations remain limited because of the assumption of circumferential symmetry. Although this model is unable to reproduce localized heating, it provides a clear and reliable picture of the global thermal response of the wheel. The model accurately captures the essential heat-transfer behavior but cannot account for geometric discontinuities or discrete block contacts.

4.1.2 Results of the 3D Model Without Brake Block

The 3D model without the brake block was generated by revolving the same 2D cross-sectional profile around the wheel axis, resulting in a fully axisymmetric 3D model. This approach is used to check the influence of dimensionality while keeping all physical and numerical parameters identical to those used in the 2D simulation. Both models share the same geometry, material properties, thermal boundary conditions, and mesh refinement in the heat-affected region, with identical circumferentially uniform heat flux applied on the tread. Under these equivalent conditions, the steady-state temperature distributions of the two models are expected to coincide; however, the 3D analysis needs more computational time due to the larger number of elements and nodes.

The results of simulations on 2D and 3D models showed excellent agreement, as shown in table 4-1. This confirms that when models are exposed to identical thermal loads and boundary conditions, they converge toward the same temperature distribution.

Temperature Result (steady-state)	Minimum(℃)	Maximum(℃)	Average (℃)
3D	367.9	706.88	486.27
2D	368.46	706.23	486.44

Table 4-1: Result of steady state and axisymmetric in 2D&3D geometry of rail wheel.

To verify the consistency between the 2D and 3D axisymmetric steady-state results, a cross-section of the 3D model was extracted at the corresponding angular position and compared directly with the 2D temperature profile. Figure 4-1 shows this comparison clearly.

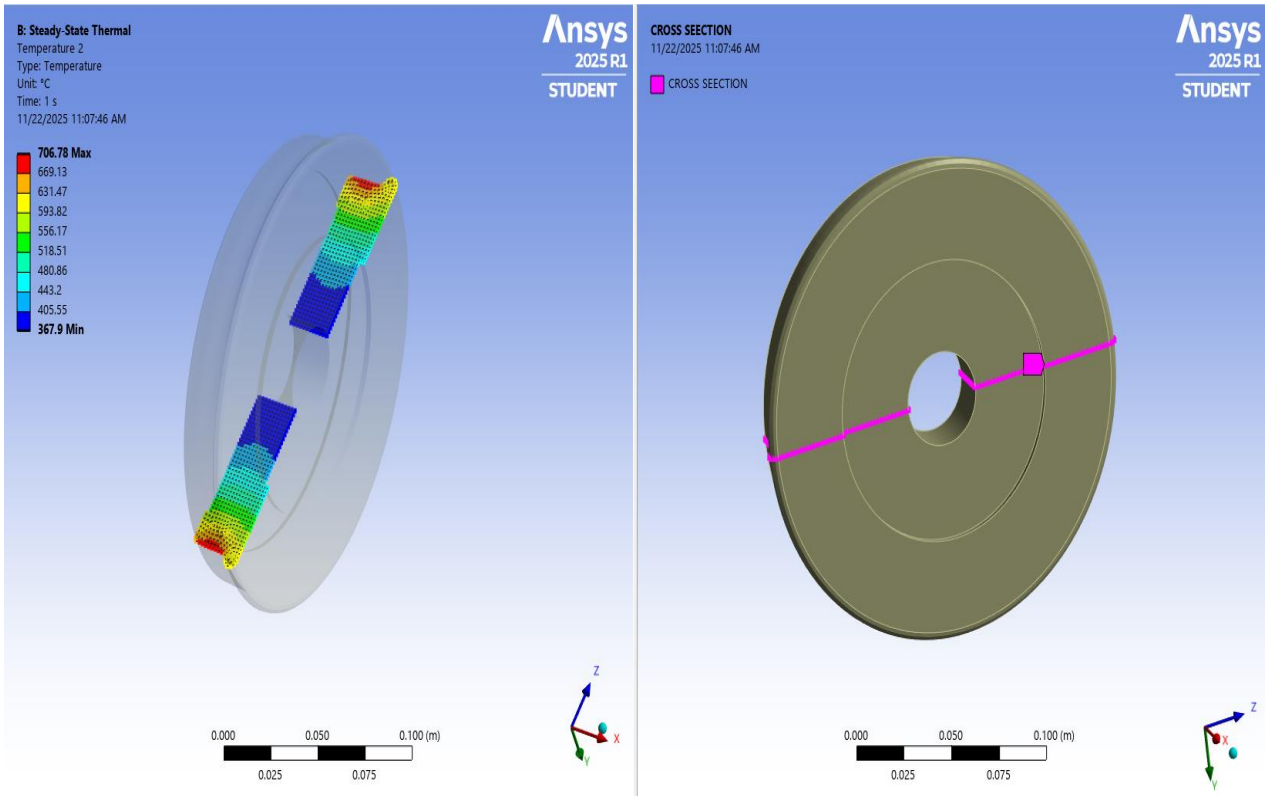

Figure 4-1: Radial cross-section extracted from the 3D model

4.1.3 Results of the 3D Model with Brake Block

The most realistic simulation of the braking process is a 3D model, including the brake block. In this configuration, heat is applied over the actual block-wheel contact area, while the brake block is acting simultaneously both as a source of heat and as a conducting path. After incorporating the blocks into the simulation, the maximum temperature increases significantly compared to the cases described above. This phenomenon happens because highly localized heat input at the block-wheel contact interface concentrates the thermal load over a much smaller area, has less potential for heat dissipation, and hence shows up with the development of a much sharper temperature peak in the contact area.

The temperature field becomes strongly non-uniform (non-axisymmetric), with localized hotspots along the block–wheel interface and showing gradients in both the radial and circumferential directions. This model captures the complex local temperature that cannot be reproduced by axisymmetric approaches. For these mentioned reasons, the 3D block-inclusive simulation represents the most accurate description of the braking scenario. A comparison of the two 3D models is provided in table 4-2.

Temperature Result(steady -state)	Minimum(℃)	Maximum(℃)	Average (℃)
3D without block	367.9	706.88	486.27
3D with block	224.03	1688.3	459.02

Table 4-2 : Comparison of steady state and axisymmetric in 3D geometry of rail wheel.

4.1.4 Comparative Analysis of the Three Modelling Approaches

In comparison, the three models display outstanding insight in terms of physical detail, computational cost, and suitability for the representation of real braking conditions. The 2D asymmetric model provides a reliable estimate of the mean temperature distribution and dissipation. Its simplicity also makes it ideal for preliminary assessments and for establishing baseline thermal behavior, something particularly useful when wear trends are analyzed or when simplified analytical models are calibrated.

The 3D model without a brake block naturally builds upon the 2D geometry exactly and confirms that, under uniform circumferential heating, both dimensional approaches converge to the same temperature field. However, the 3D model becomes remarkable once block-wheel contact is considered. In this model, the applied heat flux becomes strongly localized, giving rise to circumferential gradients and higher peak temperatures, features that cannot be reproduced in the framework of a 2D and 3D axisymmetric model.

This level of detail is required for mechanisms such as thermal softening, oxidation, crack initiation, and material degradation. These three models can be a set of complementary tools: The 2D model is useful for understanding the general temperature trends in the wheel and using fast parametric studies.

The axisymmetric 3D model confirms that the thermal behavior will remain consistent when the geometry is extended into three dimensions under uniform heating. Finally, the 3D model with the brake block captures the real localized contact heating, allowing direct comparison of the numerical results for wear tests and actual braking behavior.

Temperature Result (steady-state)	Minimum(℃)	Maximum(℃)	Average (℃)
2D	368.46	706.23	486.44
3D without block	367.9	706.88	486.27
3D with block	224.03	1688.3	459.02

Table 4-3 : Comparison of steady state in all models.

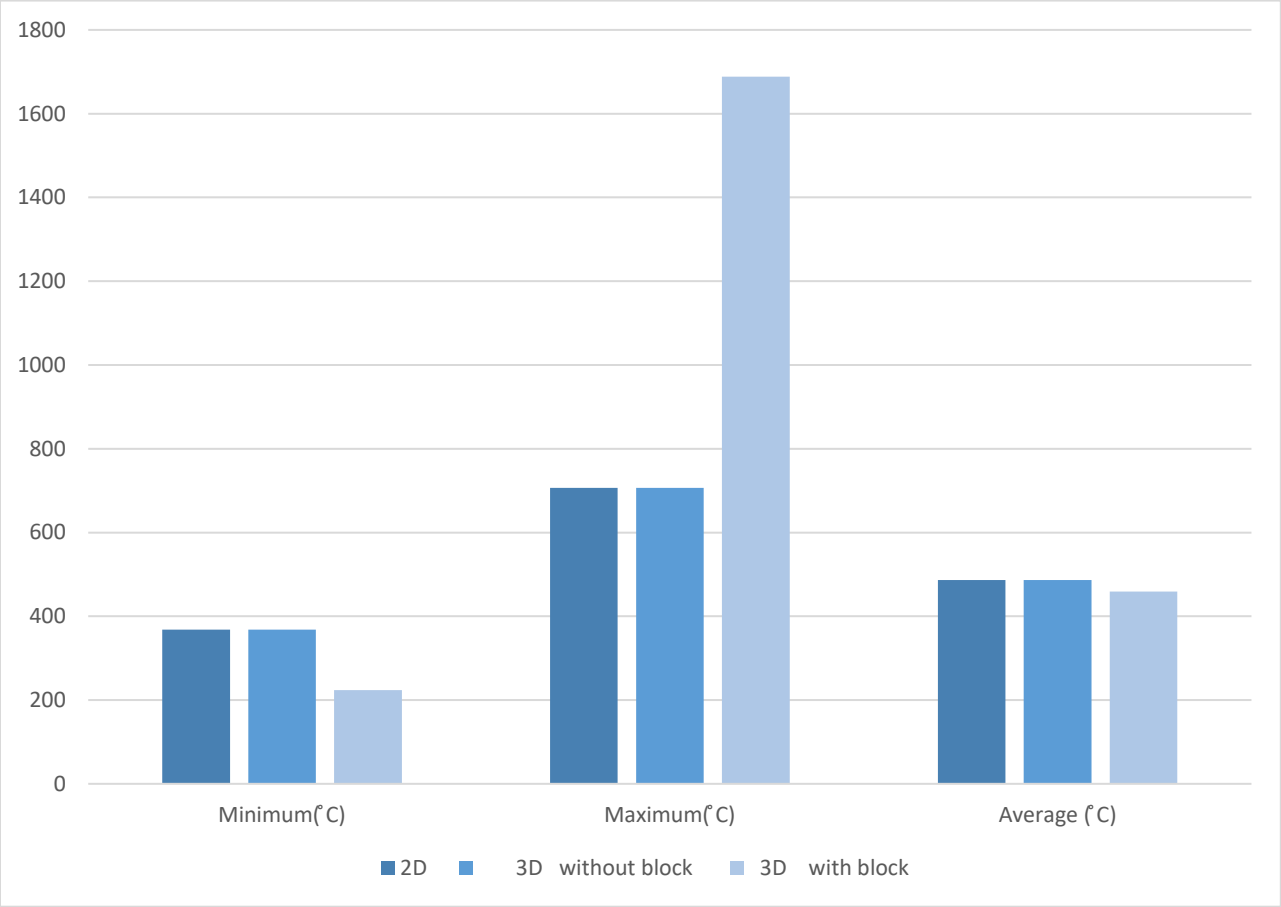

Figure 4-2 : Comparison of steady state and axisymmetric in all models.

4.1.5 Mesh Convergence

A mesh convergence study was performed for the steady-state 2D model to evaluate the influence of mesh refinement on the thermal results. The mesh convergence study involves thermal analysis several times with different mesh sizing by using the same boundary conditions and material properties. In some cases, the mesh refinement is controlled by adding several refinement levels to improve the solution. This process is repeated until a sufficiently refined mesh is obtained. As the mesh's size is reduced, the number of elements and nodes increases accordingly.

In other words, reducing the mesh size allows the solution to better represent the geometry and the heat transfer phenomena. This is especially true in regions where the temperature is varying significantly. The analysis was carried out under two cases: first, without convection, and then considering extra convection effects.

4.1.6 Mesh convergence without convection

In first case, the temperature results show a decreasing trend and reach a stable state, denoting a state of convergence for the numerical solution of the 2D steady state model.

Size (mm)	Refinement	Num elements	Num nodes	Tmin	Tmax	Tavg
5	NO	74	265	445.36	846.88	599.11
3	NO	202	671	411.75	778.39	548.29
2	NO	453	1458	409.58	778.98	541.24
2	1	1806	5615	387.38	740.94	511.08
2	2	4059	12472	365.84	701.73	482.16
2	3	7212	22029	341.61	654.73	449.62

Table 4-4 :Mesh convergence study results for the 2D steady-state thermal analysis without convection.

The curve in Fig. 4-3 represents the convergence analysis of the temperature simulation and makes the solution independent of the number of nodes or elements. It is obvious in the convergence curves, where the temperature values reduce and converge to a stable value as the mesh density is further refined. Once the difference in temperature values between two consecutive mesh refinement steps is negligible, the solution will be considered mesh-independent. This ensures that the result obtained is a true representation of the thermal behavior, and the mesh density is not unnecessarily large.

.

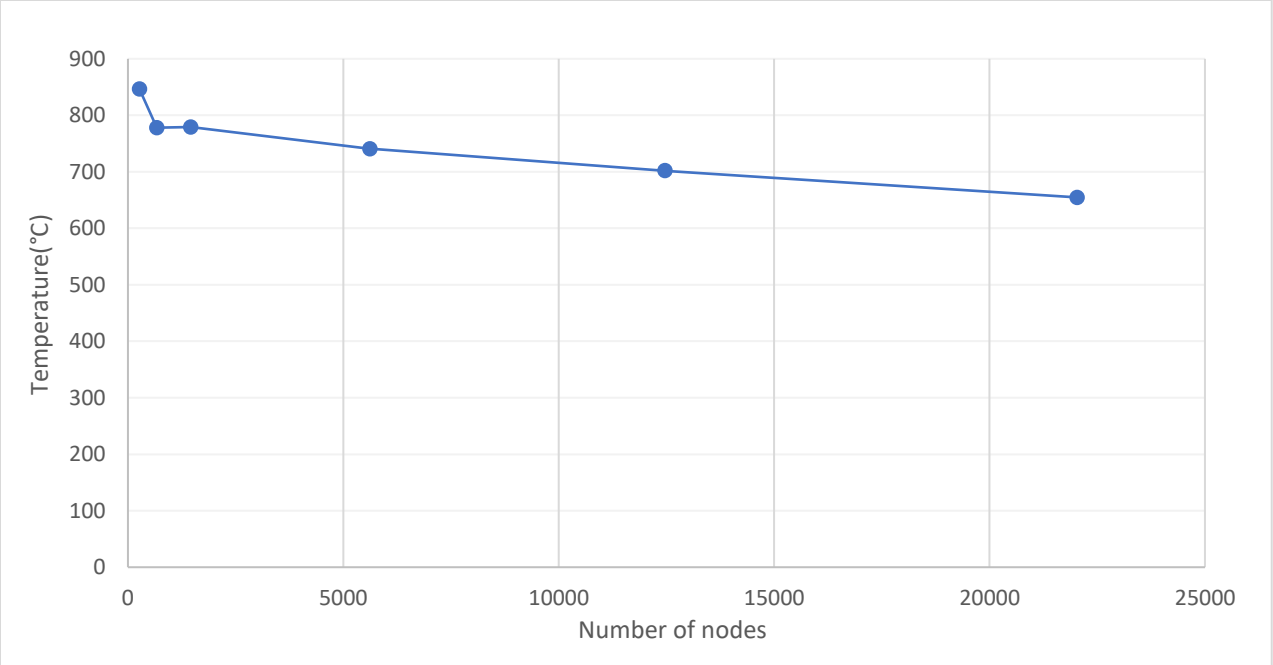

Figure 4-3 : *Mesh convergence study results for the 2D steady-state thermal analysis without convection.*

4.1.7 Mesh convergence with convection

In the second case, a named selection including two sample nodes was defined in the tread region to monitor the temperature by using the previously defined coordinate system, which is presented in fig. 4-4 and table 4-5. The mesh element size was progressively reduced to investigate the stability and accuracy of the predicted temperature values.

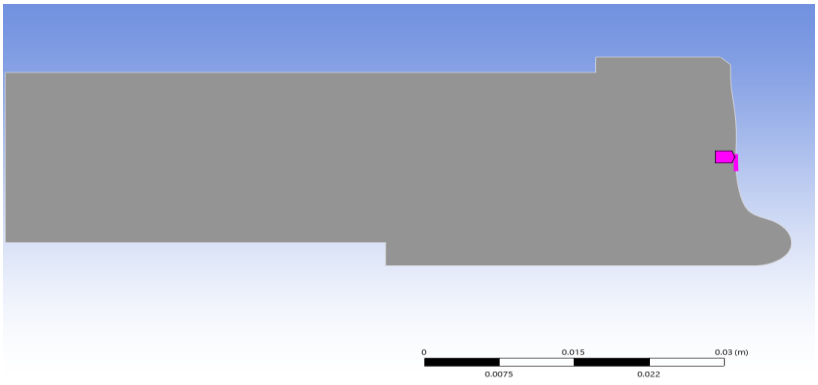

Figure 4-4: Definition of a named selection for two nodes in the tread region.

Action	Entity type	Orientation	Operator	Unit	Value	Lower bound	Upper bound	Coordinate system
Add	Mesh node	X	Greater than or equal	m	0.092	-	-	Coordinate sys
Filter	Mesh node	Y	range	m	-	-0.001	0.001	Coordinate sys

Table 4-5: Definition of a named selection for two nodes in the tread region.

In this case an extra convection boundary condition with a film coefficient of 250 W/m²K was added on the tread edge, and then the temperature distribution for the 2D profile was measured. The obtained result is shown clearly in Fig. 4-5. Following table 4-6, as the mesh refined, the temperature reduced continuously; this result confirmed the mesh convergence behavior in the thermal solution.

Size (mm)	Refinement	Num elements	Num nodes	Tmin	Tmax	Tavg	Tnode
5	NO	74	265	332.01	634.94	444.17	622.77
3	NO	202	671	305.93	579.43	405	579.43
2	NO	453	1458	304.05	581.46	399.42	576.82
1	NO	1774	5513	295.29	567.15	387.27	562.58
2	1	1806	5615	288.25	555.34	377.98	549.01
2	2	4059	12472	272.57	526.88	356.94	522.63
2	3	7212	22029	255.26	492.96	333.72	484.44

Table 4-6 Mesh convergence study results for the 2D steady-state thermal analysis with convection.

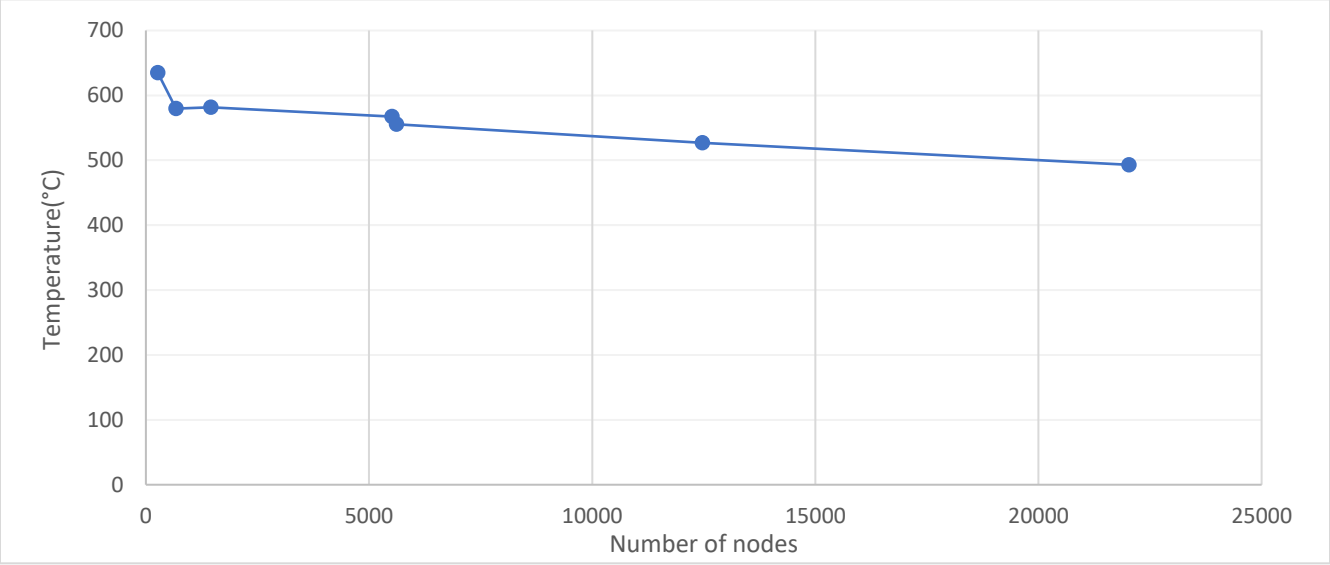

Figure 4-5: Mesh convergence study results for the 2D steady-state thermal analysis with convection.

4.2 Transient State Thermal Analysis

In addition to the steady-state evaluations performed on both the 2D and 3D axisymmetric models, a transient thermal analysis was conducted to understand how the wheel temperature evolves over time during braking. The steady-state results provide useful insight into the final thermal distribution once equilibrium is reached and the temperature distribution no longer changes with time (representing the fully developed thermal field under continuous braking); however, they do not show how quickly the wheel heats up or how the temperature propagates through the material during the braking time.

For this reason, both the 2D and 3D models were investigated under transient conditions using the same heat load, scaling laws, and boundary conditions. By comparing the time-dependent responses of the two cases, it becomes possible to assess the influence of geometry on heating rates, identify the moment when the maximum temperature is reached, and evaluate how dimensional changes affect thermal diffusion. This time-based analysis also offers essential information for wear prediction and thermo-mechanical behavior since most damage mechanisms are driven not only by peak temperature but also by the duration and speed of heating.

4.2.1 Scaling Of Time in Transient State

The transient simulation was designed to reproduce the braking conditions defined by the TSI WAG reference scenario, which specifies a standardized drag-braking operation for a 22.5-ton axle-load freight vehicle running at 70 km/h on a 21‰ downhill slope and equipped with a 2Bg cast-iron brake-block configuration. Under full-scale conditions, this braking event corresponds to a total duration of 34 minutes.

In the related research, the experimental tests used for model calibration were performed on a 1:5 scaled twin-disc tribometer. It has been done due to Pascal's similitude theory and the novel thermal scaling formulation proposed by Zampieri and Magelli [4], so the characteristic time scales with the square of the geometric scaling factor (φL^2).

Therefore, for a geometric scale factor $\varphi L = 5$, the time-scaling ratio becomes 25, and the equivalent transient braking time adopted in the numerical simulation is obtained by dividing the full-scale braking duration by this factor:

$$t_{\text{scaled}} = \frac{34}{25} = 1.36 \text{ min} \approx 82 \text{ s} \qquad (4.1)$$

This conversion ensures that the heat generation rate and thermal diffusion in the scaled simulation remain representative of the full-scale braking condition while staying consistent with the operational limits of the laboratory tribometer.

4.2.2 Transient Axisymmetric Thermal Analysis in 2D and 3D

In the transient analysis for both the 2D and 3D models, the main purpose is to examine the time dependence of the wheel temperature distribution in the same thermal loading conditions. The simulation steps remain the same as the steady-state configuration in terms of geometry, material properties, initial temperature, mesh refinement, and applied heat flux in the tread part. The only additional requirement for the transient solution is the definition of the scaled braking time and the associated time-stepping parameters, which must be consistently applied to both models to ensure a fair comparison. The only point is that in the 2D model, this was done by inserting the APDL command block as shown in fig. 4-2.

Commands

```
1  !   Commands inserted into this file will be executed just prior to the ANSYS SOLVE command.
2  !   These commands may supersede command settings set by Workbench.
3
4  !   Active UNIT system in Workbench when this object was created:  Metric (m, kg, N, s, V, A)
5  !   NOTE:  Any data that requires units (such as mass) is assumed to be in the consistent solver unit system.
6  !               See Solving Units in the help system for more information.
7
8
9  /PREP7
10 heat_flux = 8e5
11
12
13 ! --- Set initial temperature
14 allsel
15 bf,all,temp,22
16
17 ! --- Transient solution setup
18 /solu
19 antype,trans
20 time,82
21 deltim,0.1
22 autots,on
23 kbc,1
24 outres,all,all
25
26 ! --- Select nodes in Y-range on the outer surface
27 csys,12                  ! if your outer surface coordinates are defined in CSYS 12
28 cmsel,s,outer_surface,node  ! select the nodes of the component "outer_surface"
29 nsel,r,loc,y,-6e-3,8e-3  ! select nodes in Y-range
30 nlist                    ! optional: list selected nodes
31 esln                     ! select elements connected to these nodes
32 elist                    ! list selected elements
33
34 csys,0                   ! switch back to global CSYS
35
36 ! --- Apply heat flux to the correct element face
37 ! WARNING: you must verify that face 2 corresponds to the outer surface in your element type
38 sfe,all,2,hflux,,heat_flux
39
40 allsel
41
42 solve
43 finish
44
```

Figure 4-6: APDL comment for the 2D model in transient state.

The temperature distribution is calculated for the scaled time interval, as given by equation 4-1 for 82 seconds, with a time step of 0.1 seconds, and the corresponding results for the models are presented in fig.4-7 and the comparison is provided in table 4-7. The transient simulations on the 2D and 3D prove that both models exhibit an identical temperature development in time, with slight discrepancies between the minimum, maximum, and average temperatures.

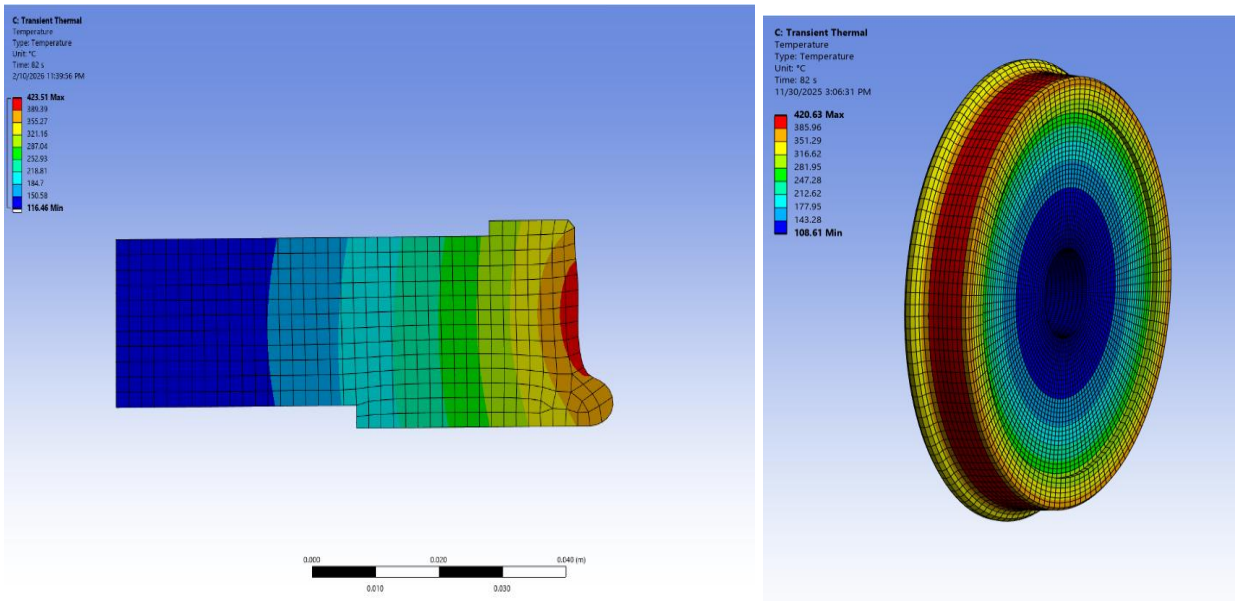

Figure 4-7: Results of the transient axisymmetric simulation on the 2D&3D rail-wheel geometry.

Temperature Result(timestep:0.1s)	Minimum(℃)	Maximum(℃)	Average (℃)	Node(℃)
2D	116.46	423.5	220.28	423.38
3D	108.78	421.3	212.7	420.31

Table 4-7: Results of the transient axisymmetric simulation on the 2D&3D wheel geometry.

The software provided the complete temperature data over the full 82-second simulation. Initially, the results were visualized directly within the software, where the maximum, minimum, and average temperatures were displayed by using different colors. However, to achieve higher resolution and clearer comparison, the temperature data were exported in Excel format. The exported data were then used to plot the trend of the maximum temperature for both the 2D and 3D models. The resulting comparison is presented in Figures 4-8 and 4-9.

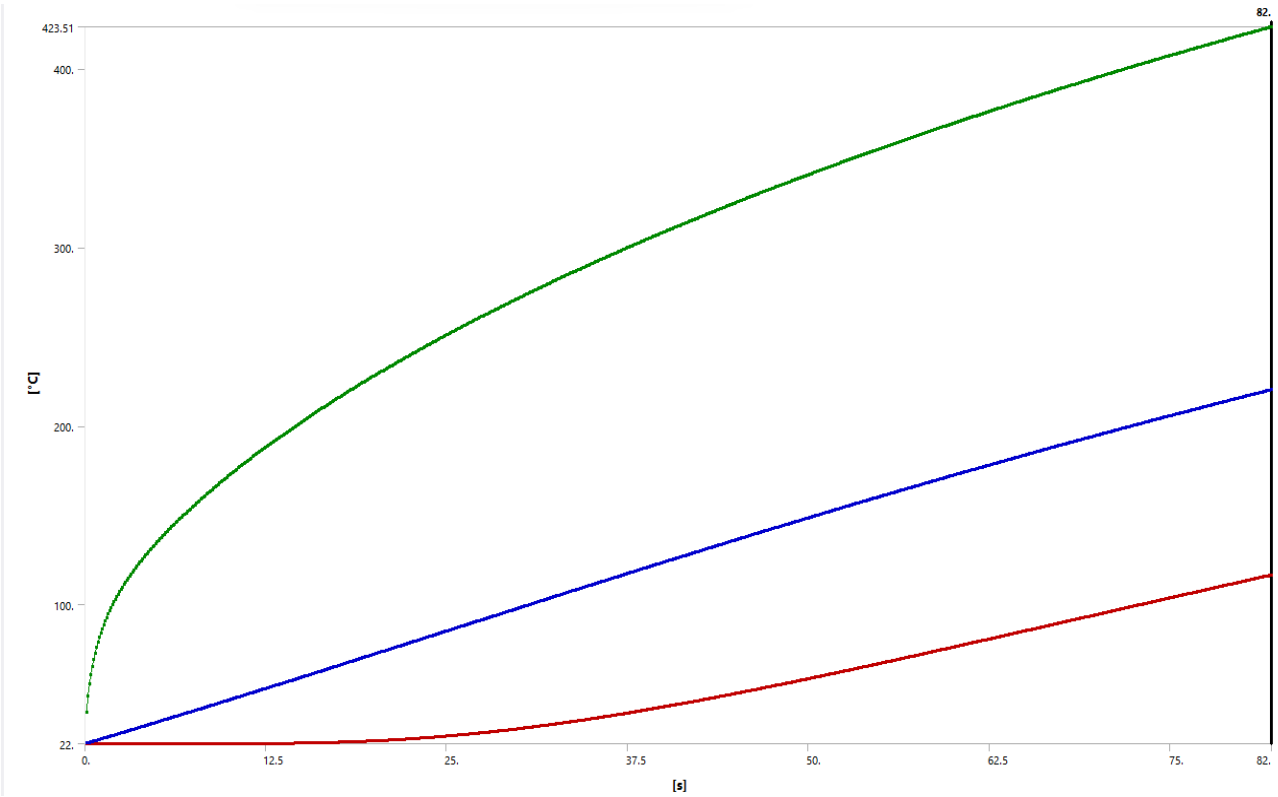

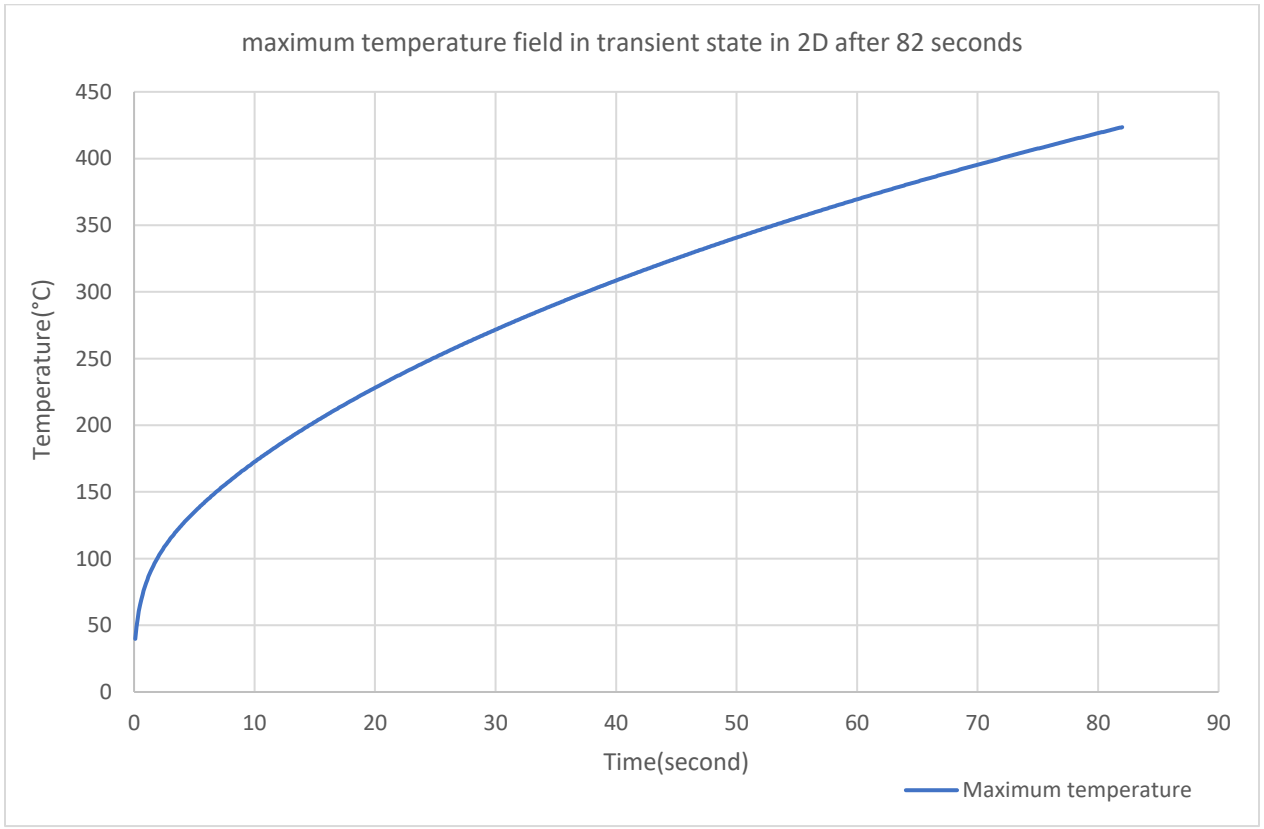

Figure 4-8: Temperature variation over time in the 2D axisymmetric transient simulation.

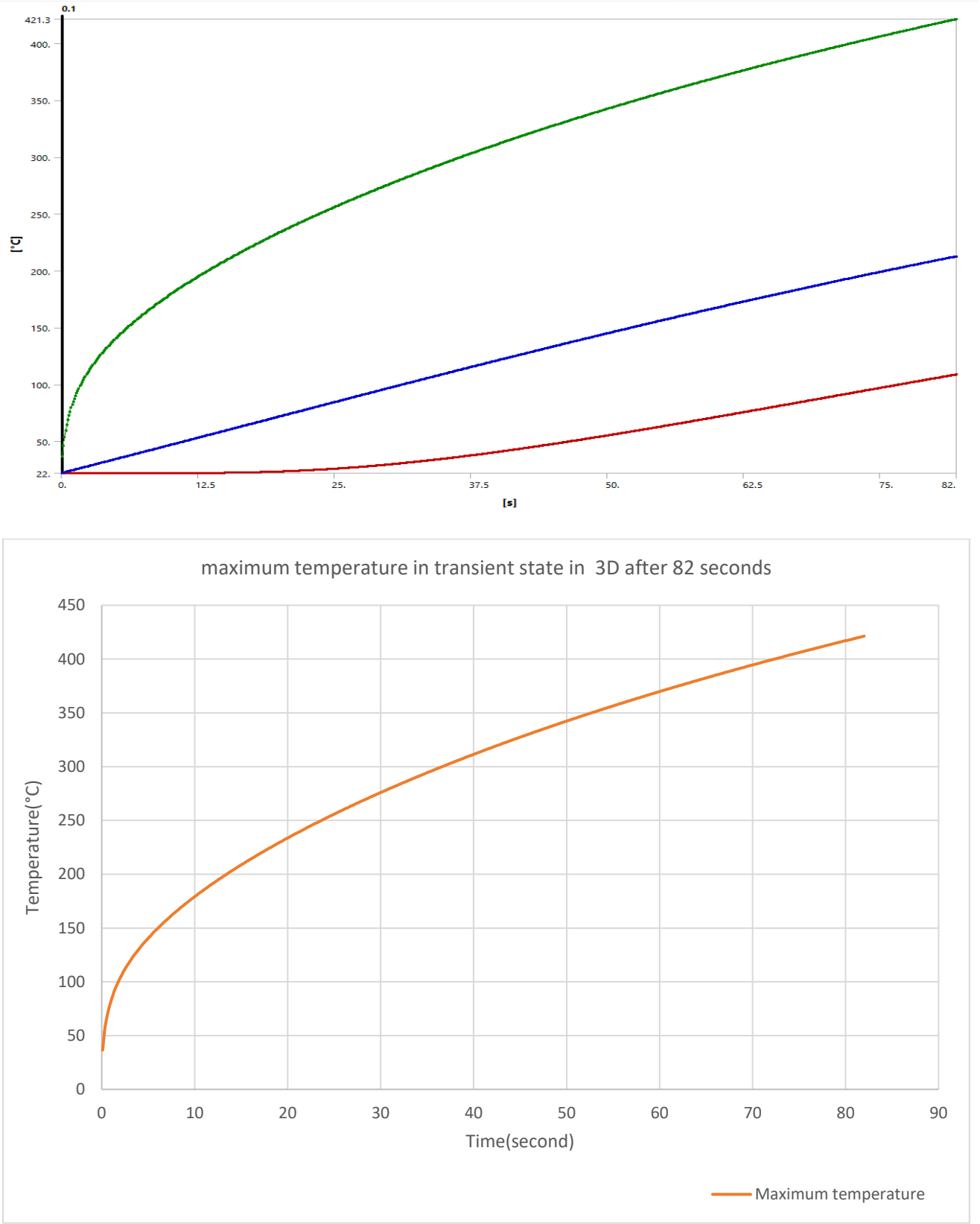

Figure 4-9: Temperature variation over time in the 3D axisymmetric transient simulation.

4.2.3 Comparison of 2D and 3D model with axisymmetric load

For a more accurate comparison in the transient state, temperature evolution for one node in the middle part of the tread was investigated as shown in fig. 4-10. It shows an identical trend and curvature during the entire simulated braking time (82 seconds). This close agreement confirms that both models are subjected to the same heat flux, scaling rules, initial temperature, and similar mesh refinement of the tread surface, and their transient thermal responses become identical during braking time. The 2D model approximates the time-dependent behavior very precisely, while the 3D axisymmetric model confirms that there are no additional dimensional effects influencing the temperature increase when heat is uniformly distributed around the wheel.

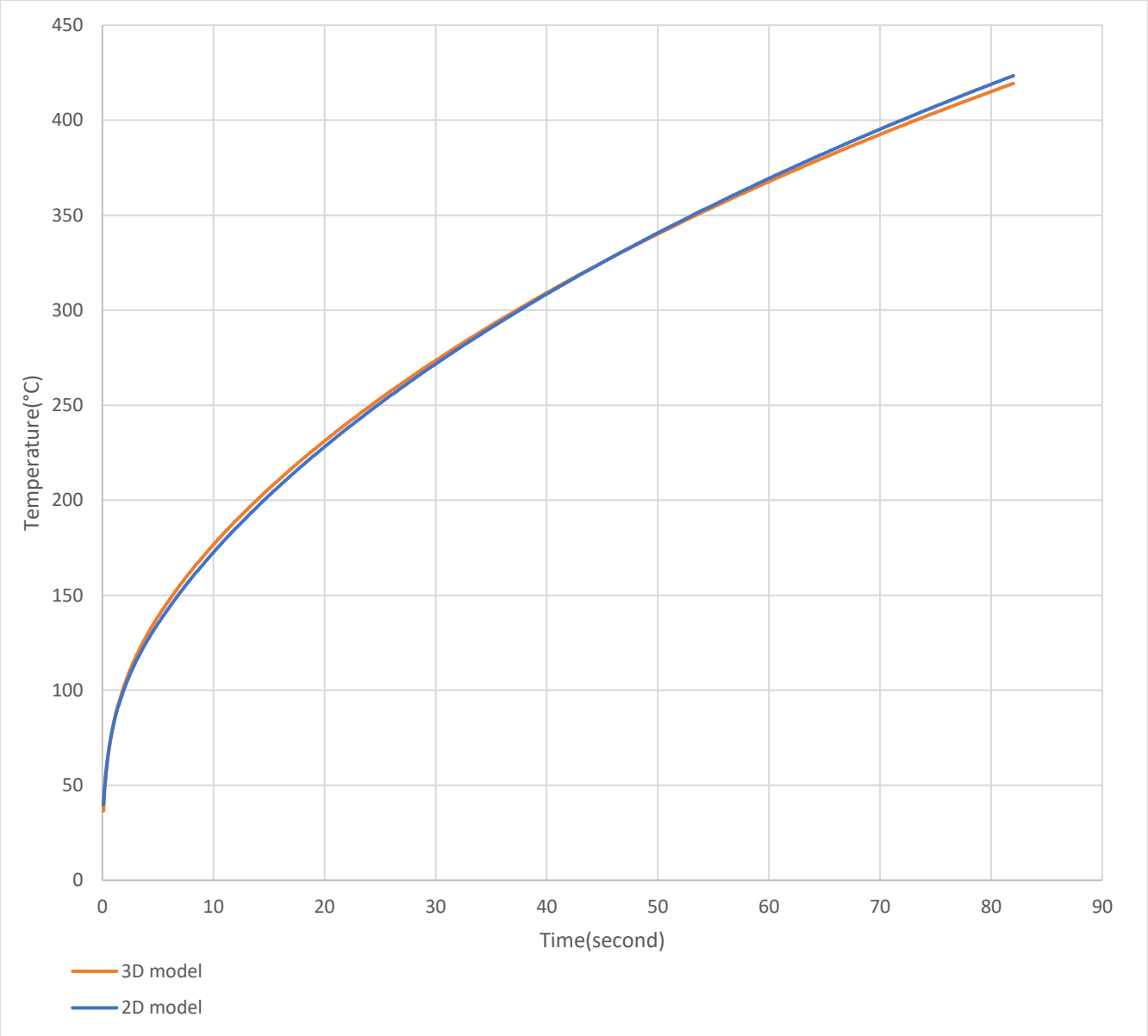

Figure 4-10: Temperature comparison of a node in an axisymmetric transient state : 2D vs 3D.

4.2.4 Transient Thermal Analysis for 3D with brake blocks

The transient simulation of the 3D model with the brake block also has been done , there is much more realistic thermal behavior, compared to the more simplified steady-state cases. The contact between the block and wheel represents a highly localized heat source, introducing frictional energy into a confined contact area. Steep temperature increases and reaching about 434°C as maximum temperature after 82 seconds which has been shown in fig.4-11.

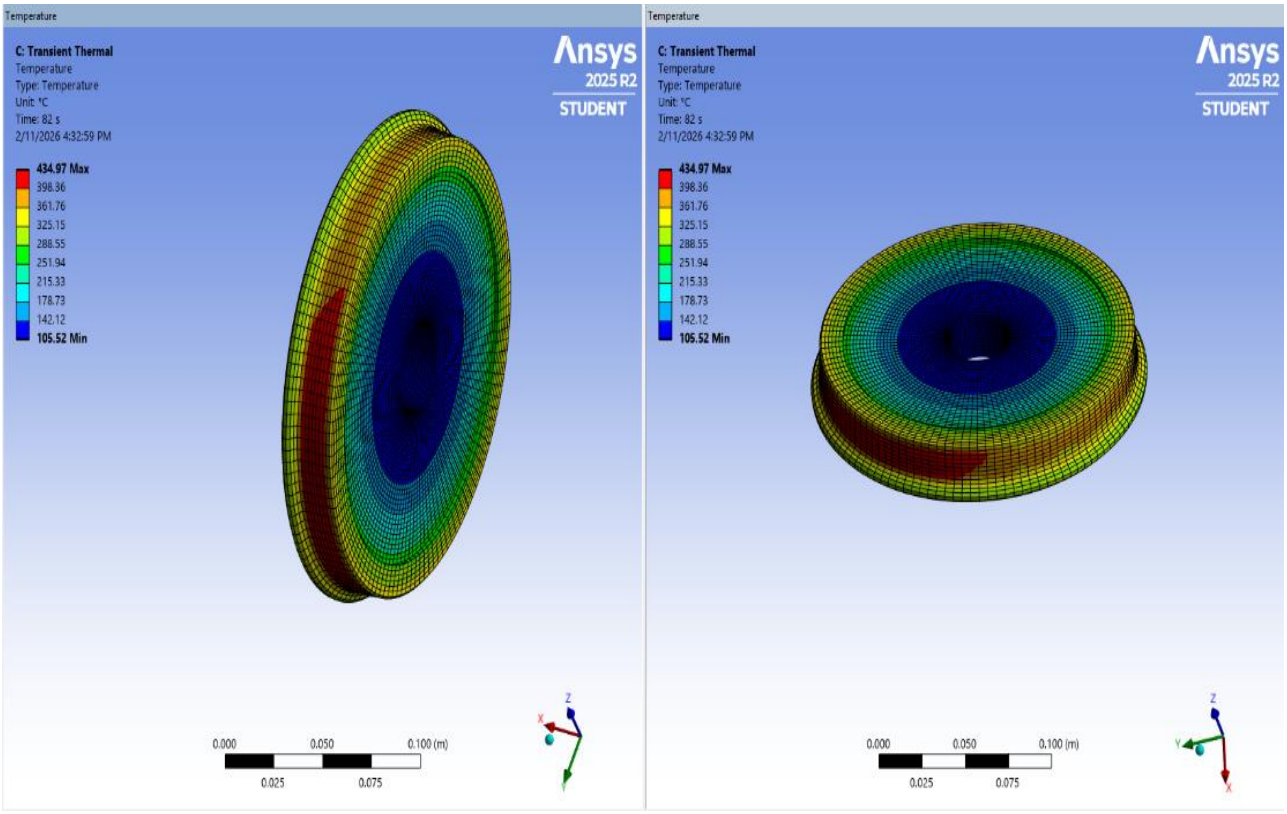

Figure 4-11: Temperature variation in 3D model with block in transient state.

The important note is that, similar to the 2D model, an APDL command was used in ANSYS Mechanical to apply rotating thermal boundary conditions during the transient simulation, as shown in Fig. 4-12. Although the wheel's material stays the same, the thermal boundary conditions vary with rotation, causing peaks and minima in temperature during each turn. Heat flux and convection loads were defined by using tabular data imported from external CSV files, allowing the loads to change with time and angular position. The heat flux distribution and convection coefficient were mapped onto the tread surface, while the ambient temperature was applied for convection. Furthermore, a cylindrical coordinate system was activated to correctly represent the circumferential variation associated with wheel rotation. This approach enabled a realistic representation of the rotating thermal loads acting on the wheel during braking.

```
/PREP7

! Define main inputs to read data

nangles = 721
Tair = 22
pippo = 10
FlussoMax = 3612832.476
ConvCoeff = 300

/INQUIRE,nlines,LINES,'C:\Users\asus\Desktop\InputFilesThesisModel\BoolTabFlux_2Bg_70kmh','CSV'
ntimes = nlines-1
! Defining table for rotating heat flux
*DIM,rotFluxData,TABLE,ntimes,nangles,1,TIME,Y,,1 !Initialization of table for heat flux (REMEMBER TO CHANGE NUMBER OF TIME POINTS)
*TREAD,rotFluxData,'C:\Users\asus\Desktop\InputFilesThesisModel\BoolTabFlux_2Bg_70kmh','CSV' ! Read the table data from CSV file (REMEBER TO SET THE CORRECT PATH)
*TOPER,rotFluxData,rotFluxData,ADD,rotFluxData,FlussoMax,0,0 ! Multiplies the heat flux
! Defining table for rotating convection
*DIM,rotConvectionData,TABLE,ntimes,nangles,1,TIME,Y,,1 !Initialization of table for convection
*TREAD,rotConvectionData,'C:\Users\asus\Desktop\InputFilesThesisModel\BoolTabConv_2Bg_70kmh','CSV' ! Read the table data from CSV file (REMEBER TO SET THE CORRECT PATH)
*TOPER,rotConvectionData,rotConvectionData,ADD,rotConvectionData,ConvCoeff,0,0 ! Multiplies the convection coefficient



! Define new ET and R sets



*GET,maxET,ELEM,0,TYPM ! Get total number of element types
*GET,maxR,ELEM,0,RELM ! Get total number of real constant sets

id_el_HF=maxET+1
id_r_HF = maxR+1
id_el_conv=maxET+2
id_r_conv = maxR+2



! Creating ET and R for heat flux elements

ET,id_el_HF,SURF152 !Define new element type set for heat flux (SURF152)
KEYOPT,id_el_HF,8,1 ! Set the new SURF elements to heat flux boundary condition
KEYOPT,id_el_HF,9,0 ! Set radiation to zero
R,id_r_HF,,0 ! Create new real constant set for h flux

! Creating ET and R for convection

ET,id_el_CONV,SURF152 !Define new element type set for convection (SURF152)
KEYOPT,id_el_CONV,8,2 ! Set the new SURF elements to convection boundary condition
KEYOPT,id_el_CONV,9,0 ! Set radiation to zero
R,id_r_CONV,,0 ! Create new real constant set for convection


CMSEL, S, tread ! Select nodes belonging to tread
ESLN ! Select elements of the current Component selection

!!!!!!!!!!! Define SURF elements for heat flux !!!!!!!!!!!
TYPE, id_el_HF
REAL,id_r_HF
ESURF, 0 ! Add the layer of SURF152 elements

!!!!!!!!!!! Define SURF elements for convection !!!!!!!!!!!
TYPE, id_el_CONV
REAL,id_r_CONV
ESURF, 0 ! Add the layer of SURF152 elements
ALLSEL


!ETLIST,4
/SOLU
csys,12

eometry  Commands
```

Figure 4-12 : APDL comment for 3D with block in transient state.

In contrast to the steady-state simulations, which are based on continuous and uniform heating until thermal equilibrium is achieved, the transient analysis resolves how the heat forms over time and how fast the temperature develops under realistic braking conditions. It showed in Fig. 4-13 that there is a nonlinear increase in the time-temperature curve, where the peak temperature rises steadily, indicating the transient effects, localized heating in wear predictions, and material degradation studies. The inclusion of the brake block within the simulation has improved more accurate modeling of the temperature field in the localized heated block-wheel contact area. Based on the results obtained, figs. 4-13 and 4-14 show the temperature distribution across the entire wheel, as well as at a single node located at the center of the tread.

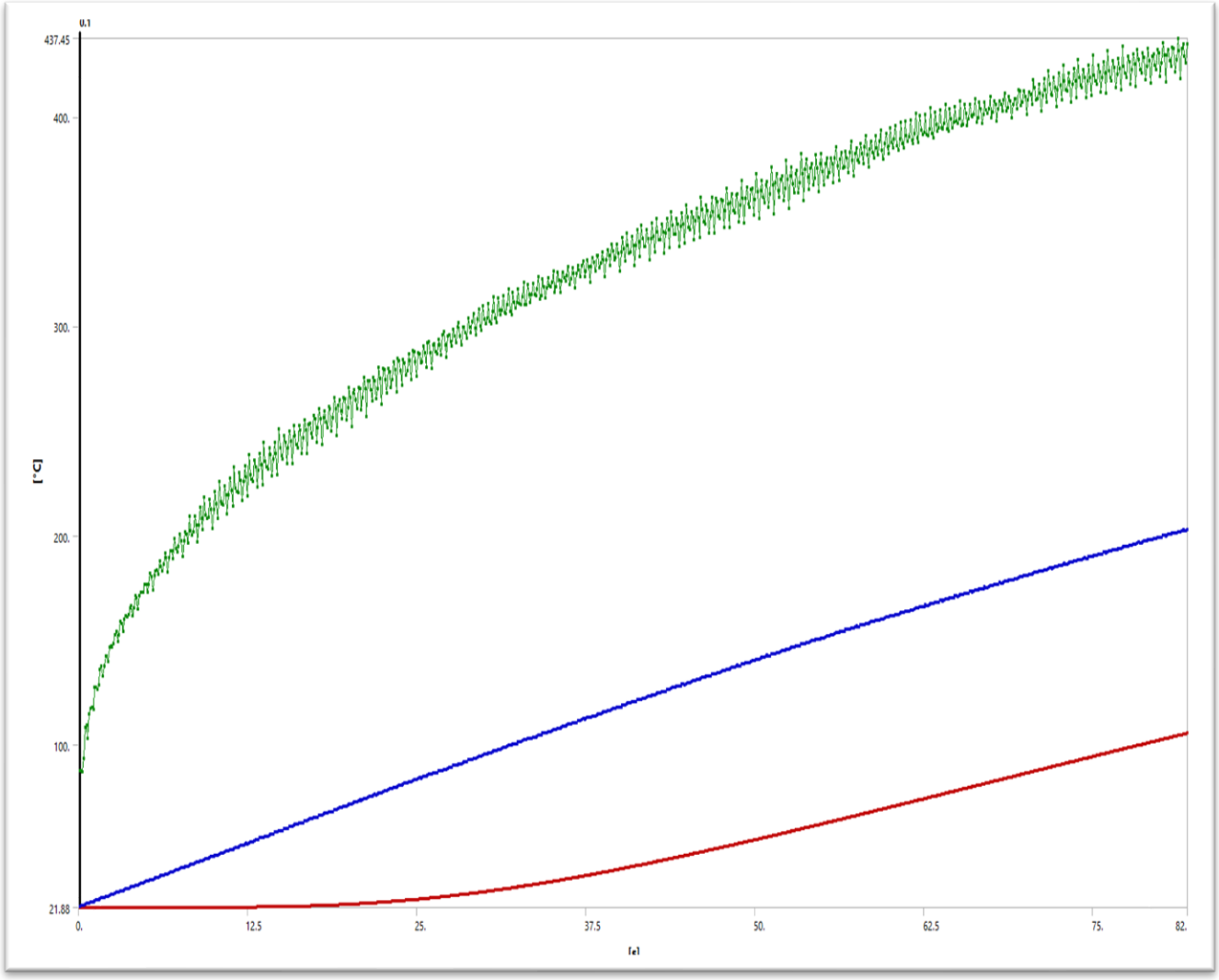

Figure 4-13: Temperature variation for3D with block in transient simulation.

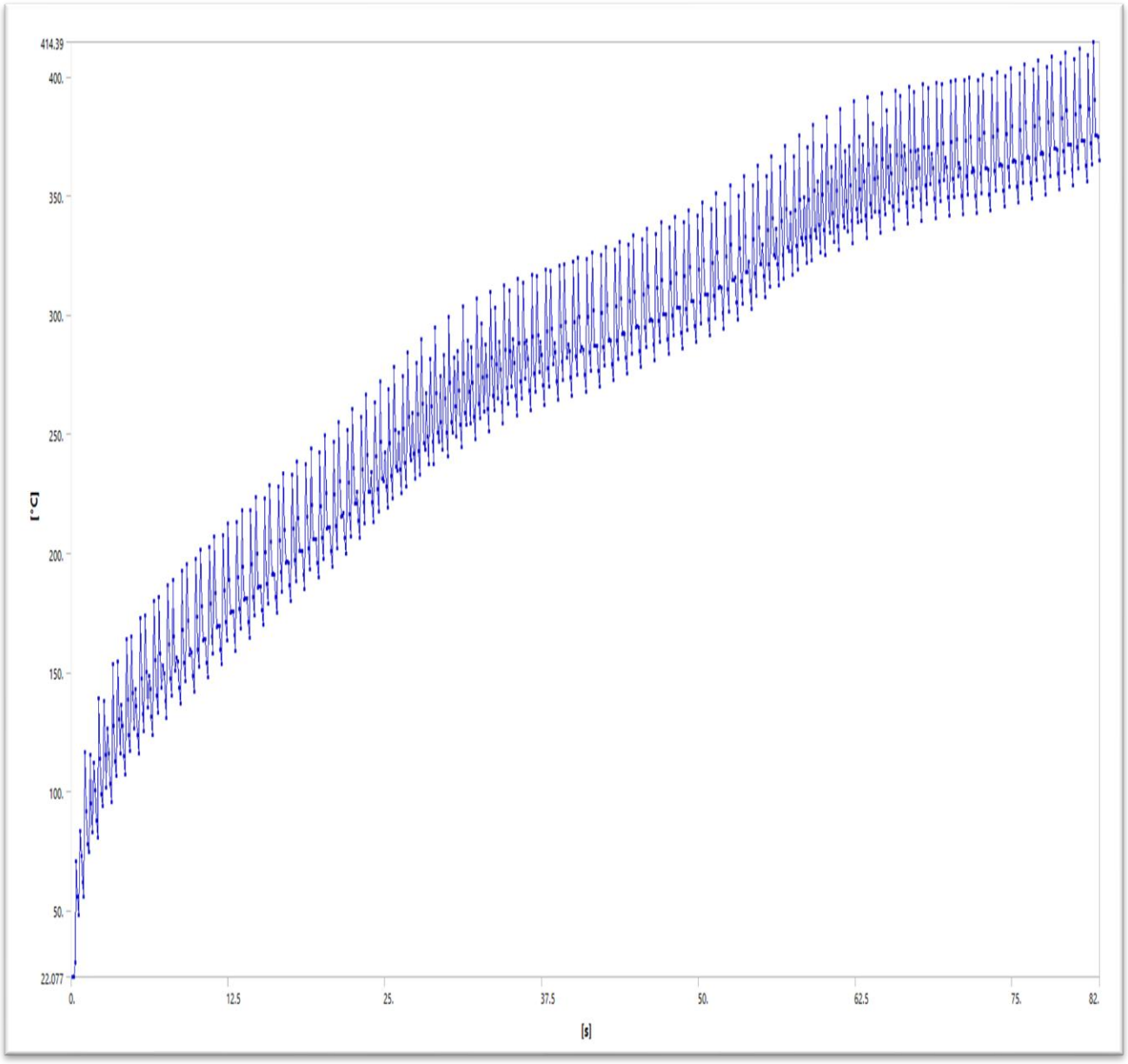

Figure 4-14: Temperature variation at a single node in the 3D model with block.

Higher-resolution plots were created from the exported ANSYS data in Fig. 4-15, showing a clear comparison between the temperature trends across the whole wheel and the temperature at the central tread node. The results show that the temperature of a node has higher fluctuations due to the brake block and localized heating area, while the wheel temperature follows a smoother trend. Despite these differences in magnitude and oscillation, both curves have a similar increasing trend over time, indicating consistent thermal behavior between the local and global responses of the wheel under braking conditions.

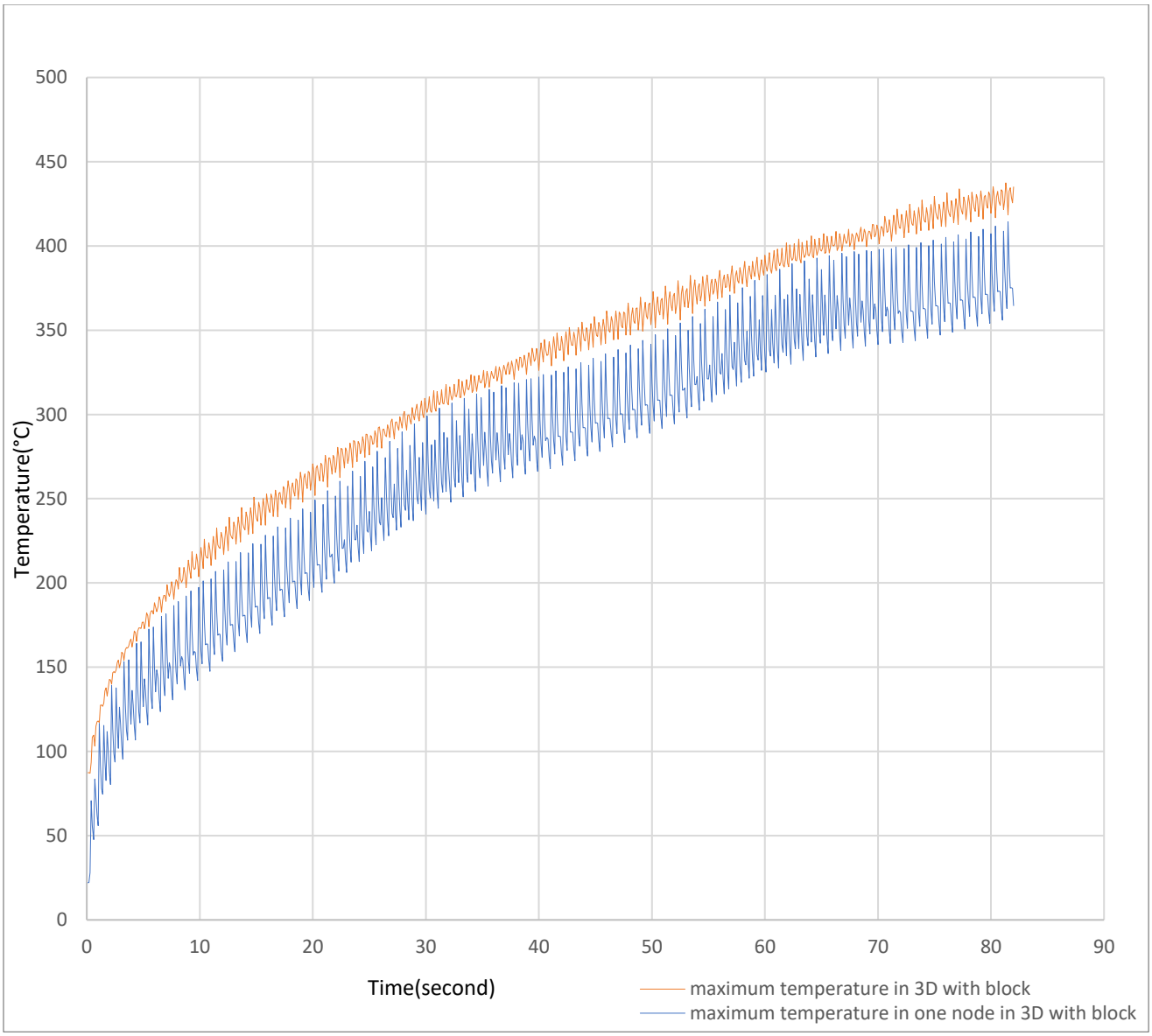

Figure 4-15: Comparison between the maximum wheel temperature and the temperature of a node in the 3D model with block.

The plot compares the maximum temperature of the entire wheel with the temperature of a specific node in the 3D model, including the brake block. The maximum temperature curve is smoother and slightly higher because it represents the hottest point among all nodes of the wheel at each time step. In contrast, the temperature of the selected node shows strong oscillations. This issue occurs because the wheel is rotating continuously and the specific node enters and leaves the contact region of the brake block. Friction causes the node to heat up when it moves under the block, and convection cools it down when it moves away. As a result, the node temperature fluctuates while the overall maximum temperature of the wheel has a smoother increasing trend.

4.2.5 Comparison of 3D model in transient state

A comparison of the temperature variation over time in the 3D transient simulations is presented in Fig. 4-16 for both 3D models. The results clearly show that in the 3D model with a brake block, the minimum and average temperatures slightly reduced, while there was an increase in the maximum temperature from 421.3 °C to 434.9 °C. The temperature curves show a consistent trend over time; the simulation including the brake block indicates higher peaks and more fluctuations due to the localized thermal load. This confirms the significant influence of the brake block on the transient state. The transient 3D model with the brake block reveals a much more critical and localized thermal response compared to the steady-state simulations, which distribute the thermal load along the tread. The temperature at the block–wheel interface rises extremely quickly. This occurs because real braking concentrates frictional energy into a small contact zone, drastically reducing heat dissipation and producing steep radial and circumferential thermal gradients.

Temperature Results (time step:0.1s)	Minimum(℃)	Maximum(℃)	Average (℃)
3D without block	108.78	421.3	212.7
3D with block	105.5	434.9	203.03

Table 4-8: Comparison of temperature variation over time in the 3D transient simulation.

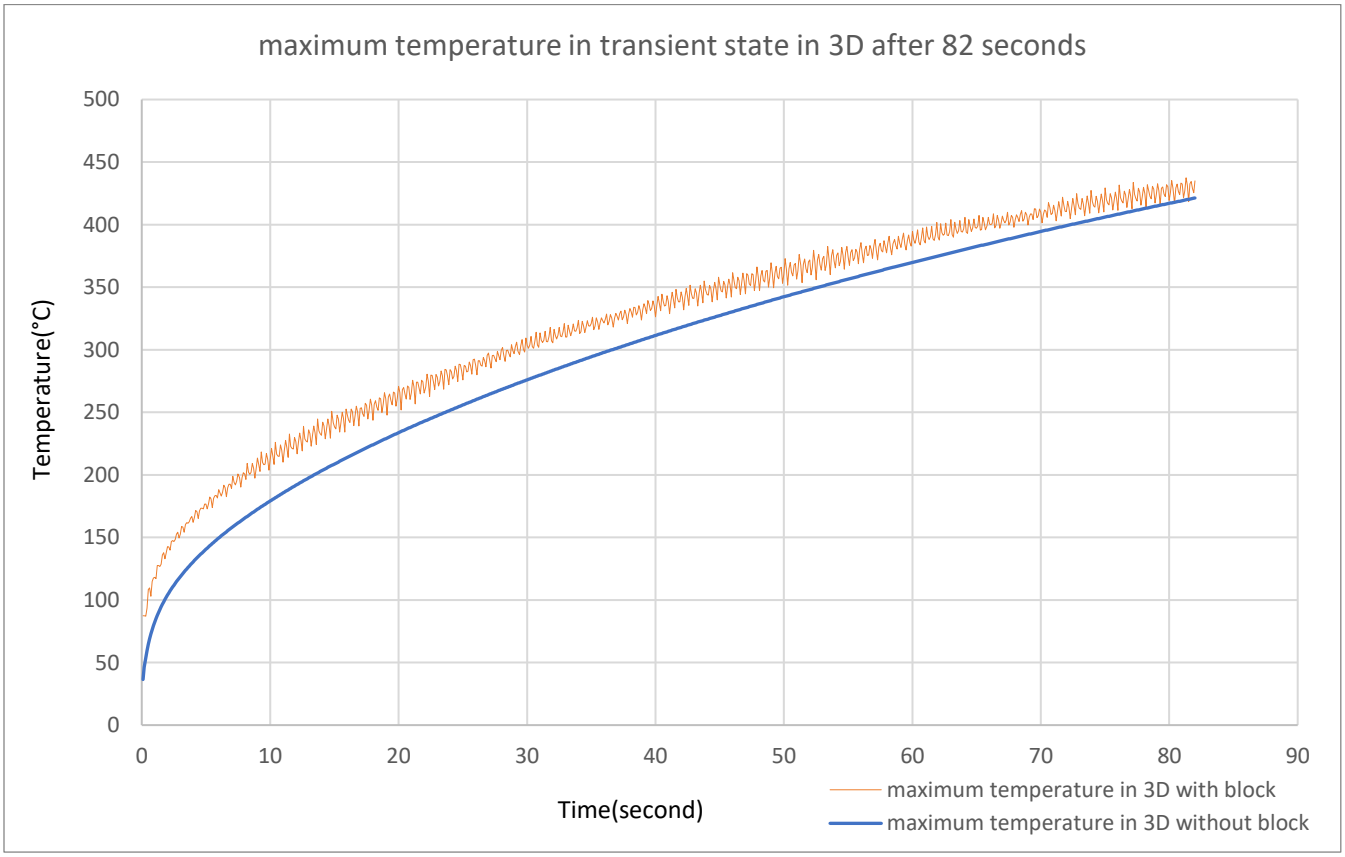

Figure 4-16: Comparison of temperature variation over time in the 3D model transient simulation.

4.2.6 Comparison of models in transient state

In order to provide a clearer comparison between the different numerical approaches in transient conditions, the temperature evolution obtained from the three models is illustrated in figure 4-17. The plot shows the variation of the maximum temperature across the wheel during the braking process for the 2D axisymmetric model, the 3D axisymmetric model, and the 3D model including the brake block. The results correspond to a transient simulation done with a time step of $\Delta t = 0.1$ s over a total braking duration of 82 seconds. This comparison allows the evaluation of the differences in thermal response using simplified and more detailed modeling approaches, highlighting the influence of the geometric representation and heat-flux distribution on the predicted temperature evolution during braking.

Temperature Results (time step:0.1s)	Minimum(℃)	Maximum(℃)	Average (℃)	T_{node}(℃)
2D	116.46	423.5	220.28	423.38
3D without block	108.78	421.3	212.7	420.31
3D with block	105.5	434.9	203.03	431.5

Table 4-9: Comparison of temperature variation over time in the transient simulation.

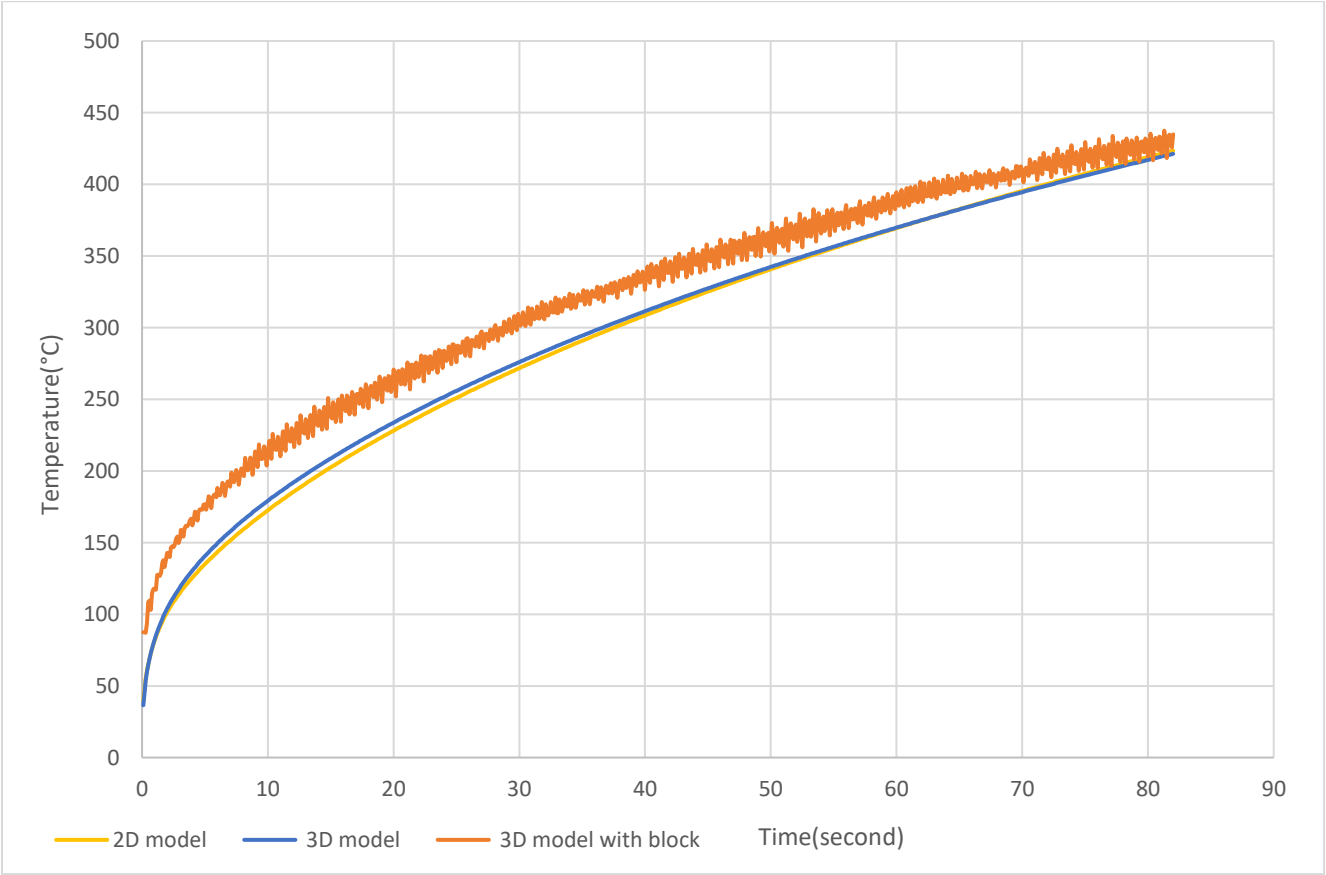

Figure 4-17: Comparison of Temperature variation over time for all models in the transient simulation.

4.3 Effect of time step in transient state of 3D with block

This analysis was performed to evaluate the influence of time stepping on the accuracy and stability of the transient thermal simulation by defining different time steps in 30 seconds. Simulation time is reduced instead of a full-scale model (82 seconds) to obtain results more quickly. In this approach, different time-step sizes from the lowest to the highest amount were examined and compared in terms of the temperature response. This simulation was performed on a 3D model, including the brake block and non-axisymmetric thermal load, which provides the closest representation of real braking conditions.

4.3.1 Time stepping effect in non-axisymmetric model

In this case, larger time steps, like $\Delta t = 1$ s, tend to produce less accurate peak predictions and a more irregular temperature evolution because, for this large time step, it is hard to properly capture the repeated heat input. In contrast, smaller time steps provide more stable and consistent peak estimates, with smoother oscillatory behavior. As shown in Fig. 4-18, the smallest time step, $\Delta t = 0.001$ s, appears significantly smoother because the adopted time step is much smaller than the wheel rotation frequency. In table 4-10, the minimum and average temperatures remain consistent across all time steps, indicating that the global thermal response is not significantly affected by the time increment. However, noticeable differences appear in the maximum temperature values.

Time Step	Minimum(℃)	Maximum(℃)	Average (℃)	T_{node}(℃)
0.001	29.478	268.83	94.917	258.36
0.05	29.499	290.56	95.009	256.96
0.1	29.495	303.58	95.358	240.73
0.5	29.186	378.54	96.063	229.89
1	30.176	415.26	94.331	256.8

Table 4-10:Comparison the effect of time step in the 3D model with block transient simulation.

The maximum temperature plot, which provides fig. 4-18, confirms this observation for the 3D model with a non-axisymmetric load for different time steps. All curves in this plot exhibit an increasing temperature trend; coarser time steps result in more pronounced fluctuations and peak overestimations. As the time step decreases, the temperature evolution becomes more refined and physically consistent. Similar behavior is observed at the middle node of the tread in fig. 4-19, although the fluctuations are more pronounced due to the localized contact area of heat flux. The higher time step is unable to accurately capture the rapid thermal oscillations associated with wheel rotation, while lower time steps provide a more stable and physically consistent temperature evolution.

In general, the comparison confirms that a time step significantly affects the predicted thermal peaks, especially in localized regions. Smaller time increments improve numerical stability and accuracy, ensuring more reliability in the transient thermal behavior of the tread-braked wheel. Therefore, the smallest investigated time step, $\Delta t = 0.001$ s, was selected as the most suitable value to ensure the numerical stability of the adopted method.

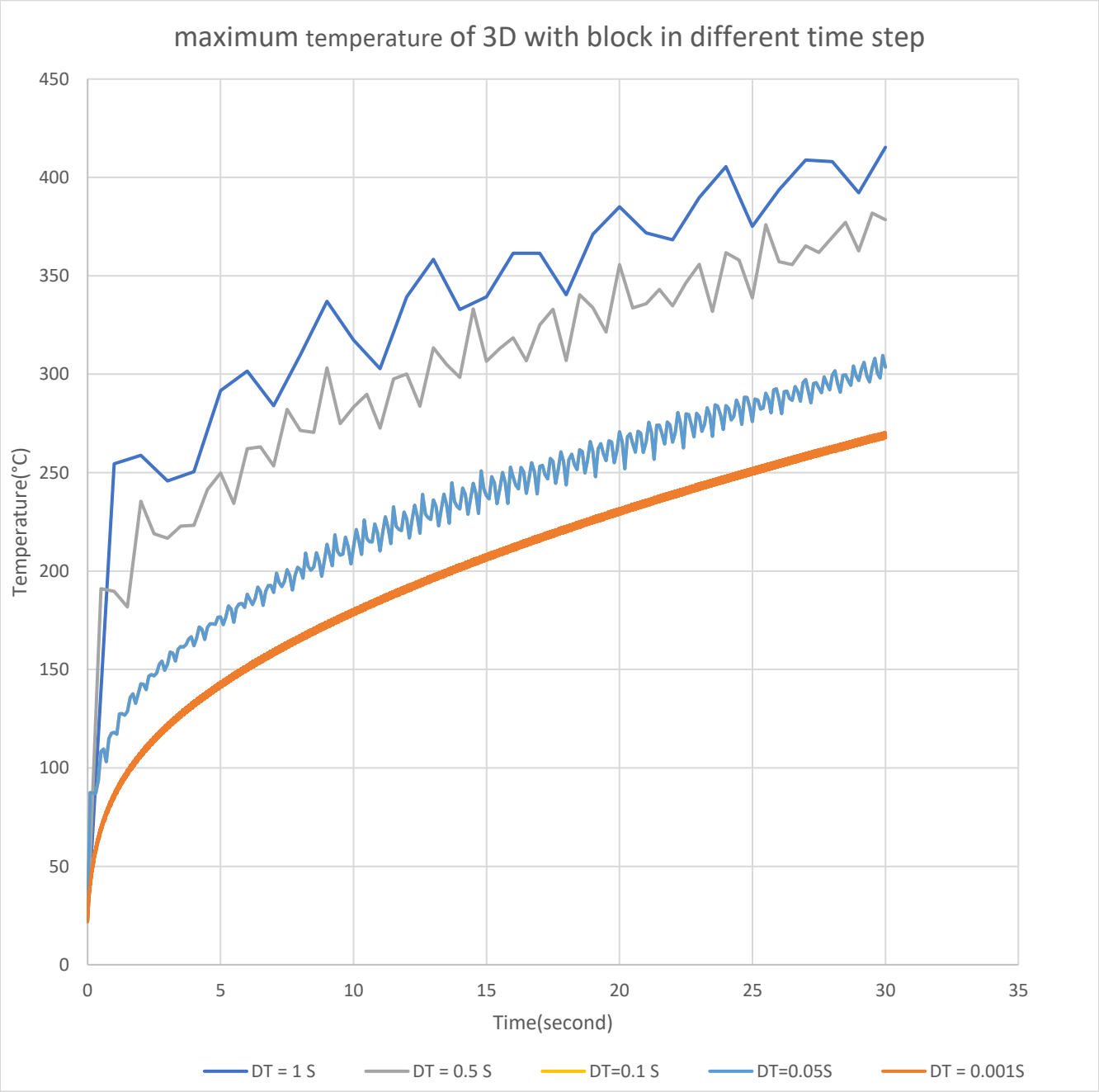

Figure 4-18: Comparison of time- stepping effect on maximum temperature in the 3D model with block .

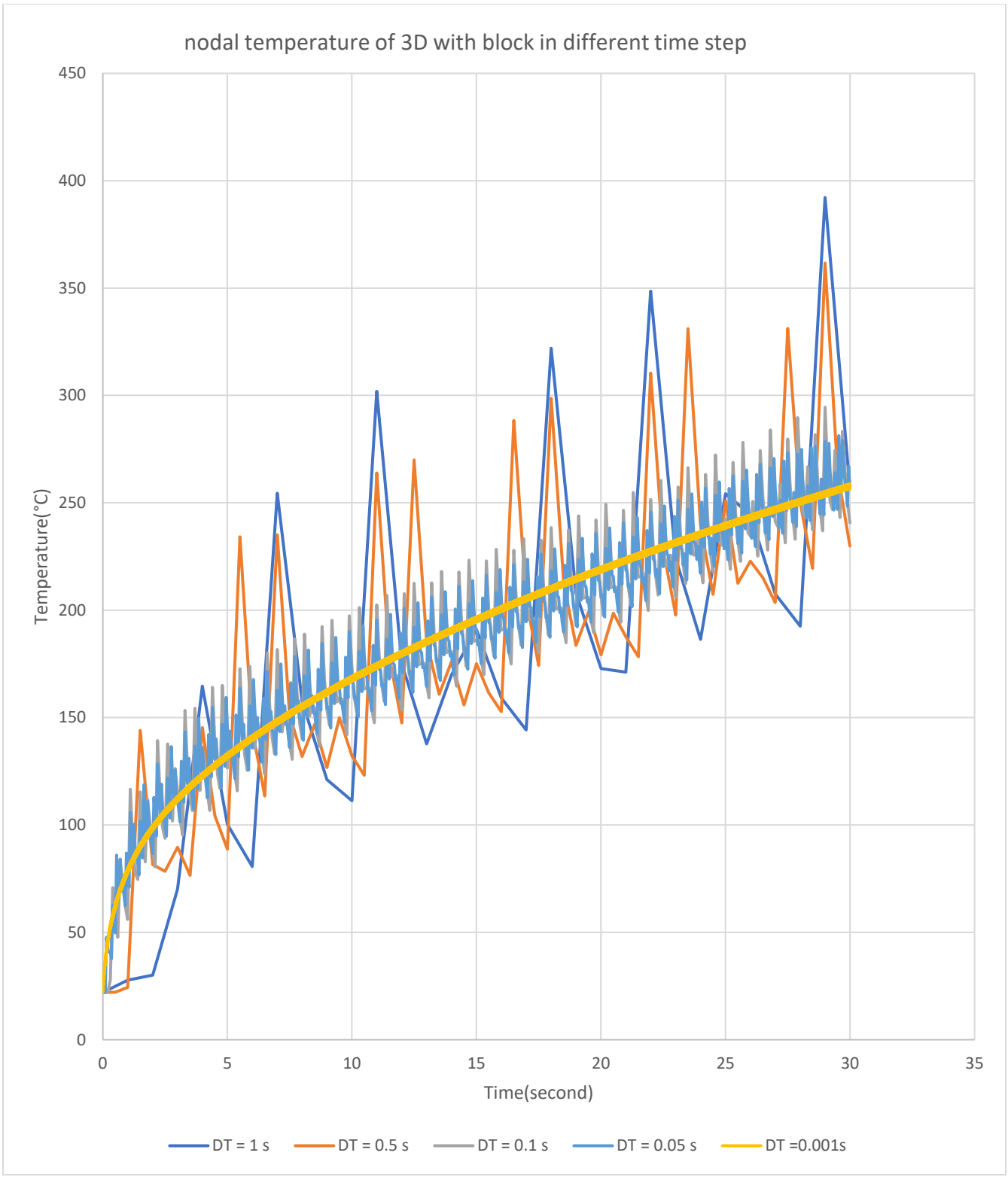

Figure 4-19 : Comparison of time- stepping effect on nodal temperature in the 3D model with block.

4.3.2 Transient Temperature Comparison for Different Models

For a clear comparison of the transient thermal behavior across the different physical models, the analysis was performed using the smallest investigated time step, $\Delta t = 0.001$ s, which provides the highest numerical stability and temporal resolution. The temperature distribution was evaluated for all considered models, including the 2D axisymmetric model; the 3D axisymmetric model with an axisymmetric thermal load; and the 3D model including the brake block (non-axisymmetric). The comparison was provided after 30 seconds of braking under the imposed heat flux and wheel rotation conditions. The corresponding temperature values obtained from the simulations are reported in Table 4-11, and the temperature evolution at a selected node on the tread is shown in Figure 4-20.

Time Step=0.001s After 30 seconds	Minimum(℃)	Maximum(℃)	Average (℃)	T_{node}(℃)
3D with block	29.478	268.83	94.917	258.36
3D without block	29.347	265.47	94.231	255.57
2D	29.245	264.31	94.079	254.32

Table 4-11:Comparison of the effect of time step size in all models.

As shown in Figure 4-20, the temperature trends predicted by the 2D axisymmetric model and the 3D axisymmetric model are almost identical, since both approaches assume a uniform circumferential distribution of the thermal load along the wheel tread. Under these axisymmetric conditions, the physical problem is rotationally symmetric, and therefore, both numerical formulations reproduce the same thermal response. Only small differences can be observed, which are related to numerical discretization and mesh effects. In contrast, the 3D model including the brake block exhibits slightly higher temperatures, as the heat flux is applied locally over the contact region between the brake block and the wheel, producing a more concentrated thermal load during braking.

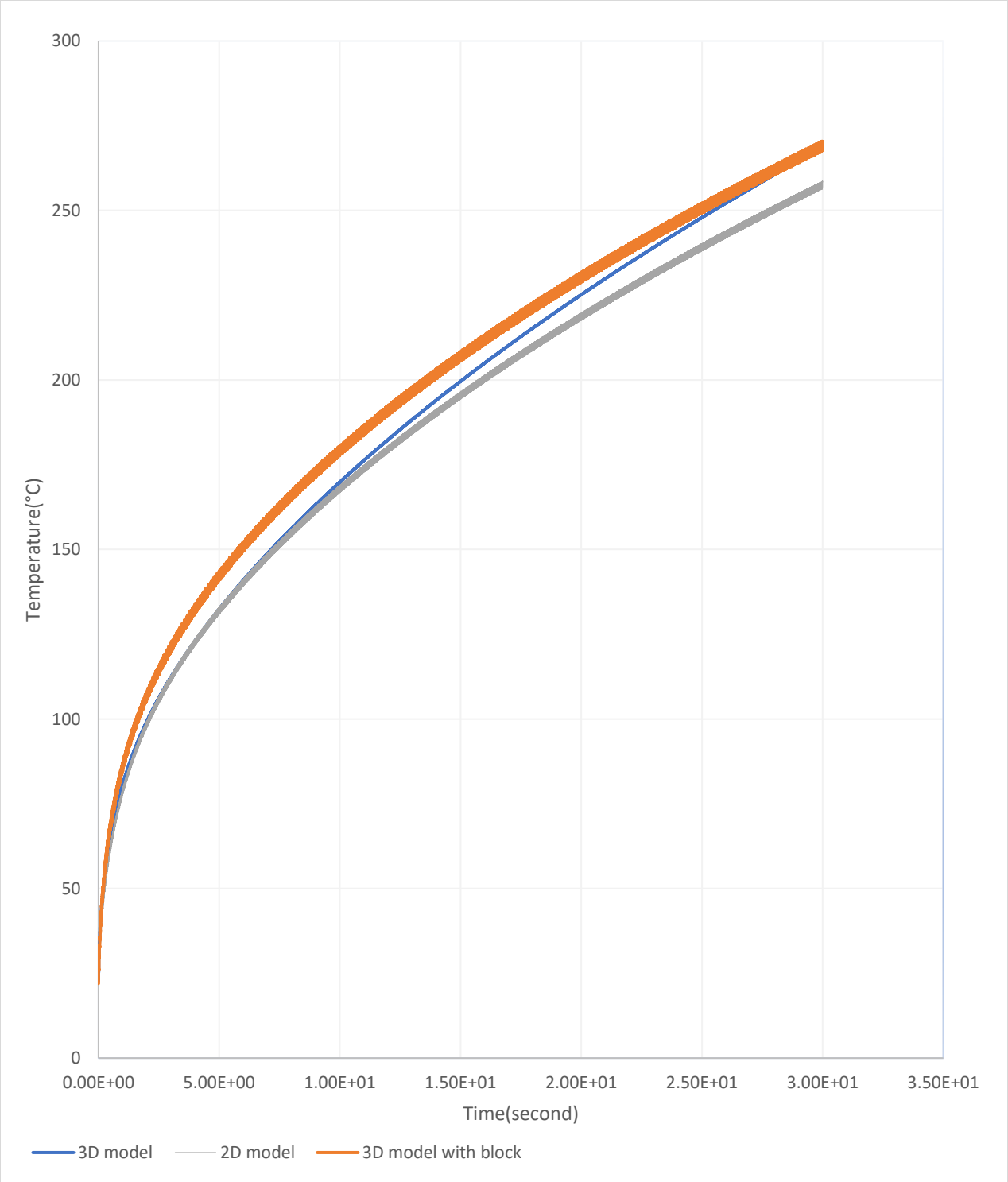

Figure 4-20: Comparison of a nodal temperature for all models in transient state.

5 Future Development

Future developments of this work may concern the refinement and extension of the numerical model to make its output closer to the real thermo-mechanical behavior of wheel-block braking. The first necessary step would be a full thermo-mechanical simulation; this simulation can account for the effects of deformation, thermal expansion, and evolution of contact pressure during braking. [1] [17] All these effects are known with the severe influence of the temperature rise, heat partitioning, and development of wear or damage. [12] A deeper understanding of how different service scenarios affect the thermal field would be obtained by exploring a wider range of operating conditions, such as sliding velocity, applied normal force, braking duration, material selection, and block-tread contact geometry variations.

One important aspect for future development follows the alternative materials for both the railway wheel and the brake block. The thermal behavior of the braking system is strongly influenced by the thermal properties of the materials. [9] For this reason, material selection with improved thermal properties could affect the temperature distribution and the wear mechanisms occurring during braking. Future studies could focus on different alternative brake-block materials to improve thermal performance and extend the service life of both the wheel and the braking components. [25]

5.1 Material Selection

The material of the brake block has a direct effect on how the heat is shared between the block and the wheel during braking. This means that choosing the right material is an important part of the thermal analysis. In this case, low thermal conductivity materials, such as organic or composite blocks, cannot effectively absorb the heat, so most of the heat generated on the contact surface is transferred to the wheel. Conversely, materials characterized by high conductivity, such as the cast iron employed in the simulation, exhibit superior heat absorption capabilities, provide stable friction, and reduce the thermal load on the wheel. But this material will degrade rapidly under high thermal loads and lead to oxidation, crack development, and accelerated wear. [11][17]

The wheel in the performed simulation was considered steel since it is more resilient and becomes vulnerable to creeping and thermal cracking when subjected to elevated temperatures. [2][3] Thermal and mechanical properties of these two materials have been shown in Table 5-1.

Property	Wheel (Steel)	Brake Block (Cast Iron)
Thermal conductivity, λ (W/m·°K)	50	48
Specific heat, c (J/kg°K)	487	560
Density, ρ (kg/m³)	7818	7100
Yield stress, σ_γ (MPa)	≈ 550 MPa	≈ 200 MPa

Table 5-1physical and mechanical properties of rail wheel and brake block.

other important aspect related to the block material include contact pressure and friction behavior. Each block type has its friction coefficient, wear response, and sensitivity to temperature [11][13]. In the performed simulation, the friction behavior explained by the Karwatzki law, which is applicable for cast-iron brake blocks [7]. Other materials, such as composite or sintered metallic blocks, will require different friction models to accurately represent their friction behavior.

5.2 Alternative Materials for Wheels and Braking Blocks

As mentioned before, severe, and prolonged heating has direct consequences on wear and structural integrity. Under long time braking, the steel wheel tread can experience creep deformation due to elevated temperatures that soften the steel and reduce its yield strength. At the same time, the combination of localized overheating and sharp thermal gradients promotes thermal fatigue, crack initiation, and propagating microcracks.[9][11] These findings proved the importance of alternative material for both brake blocks and wheels. Which can help us to improve safety and extend the service life of both components.[9][25] Recent technological and material developments recommend new brake block materials with improved properties, capable of reducing heat transfer to the wheel and minimizing wear on its surface. [26][27]

For this reason, alternative brake-block materials categorized as follows:

- Composite brake blocks with resin–metal or fiber reinforcement with reduced thermal conductivity and lower wear at high temperatures.
- Sintered friction materials, commonly used in high-speed rail systems that keep friction stability and structural integrity at higher temperatures.
- Ceramic or mineral-reinforced composites that offer improved oxidation resistance and reduced thermal fatigue.
- Advanced polymer–ceramic hybrid friction materials, with capacity to withstand rapid heating and repeated braking cycles.[26][28]

For the wheel, research in railway engineering suggests the potential benefits of bainitic steels, heat-resistant pearlitic steels, and functionally graded materials (FGMs), with great resistance to creep, thermal fatigue, and crack initiation compared with standard wheel steels.[9][10]

5.3 Heat partition factor in material selection

A key parameter in brake-block material selection is the heat partition factor, as it governs the distribution of frictional heat between the wheel and the block. The thermal absorption capacity of the block material influences the resulting temperature field during braking.[11]

As the heat partition factor (β) increases, a larger amount of frictional heat enters the wheel. This leads to higher surface temperatures and thermal gradients. These thermal effects can cause problems like hot spots, cracking, and material degradation. In railway braking studies, the heat partition factor (β) is not measured directly; it is usually calculated through analytical formulations, numerical modeling, or experimental calibration. It indicates the fraction of frictional heat that flows into the wheel, while the remaining portion is absorbed by the brake block. The frictional heat at the contact area is defined by equation 5-1:[21]

$$Q = \mu F_N v \qquad 5\text{-}1$$

where μ is the friction coefficient, F_N is the normal contact force, and v is the sliding velocity. The heat partition factor β is related to the frictional heat with below equations[2][11]

$$Q_{wheel} = \beta Q \qquad 5\text{-}2$$

$$Q_{block} = (1 - \beta) Q \qquad 5\text{-}3$$

The heat partition factor (β) is estimated using thermal contact theory, where it depends on the thermal effusivity in the materials. Thermal effusivity is defined as:[19][21]

$$e = \sqrt{k \rho c} \qquad 5\text{-}4$$

where k is thermal conductivity, ρ density, and c specific heat capacity. Under this approach, the heat partition factor can be approximated as:[11][18]

$$\beta = \frac{e_{wheel}}{e_{wheel} + e_{block}} \qquad 5\text{-}5$$

This formulation, discussed in braking literature such as Vernersson [2][3] and Kral & Vernersson [11], accounts for the different thermal absorption capacities in the materials. Materials with higher thermal effusivity absorb more heat. This parameter can be calibrated by adjusting its value in finite element simulations until the predicted temperature evolution matches experimental measurements, which are usually done in thermo-mechanical railway studies. Comparison of the heat partition factor in different material has been shown in Fig5-1.

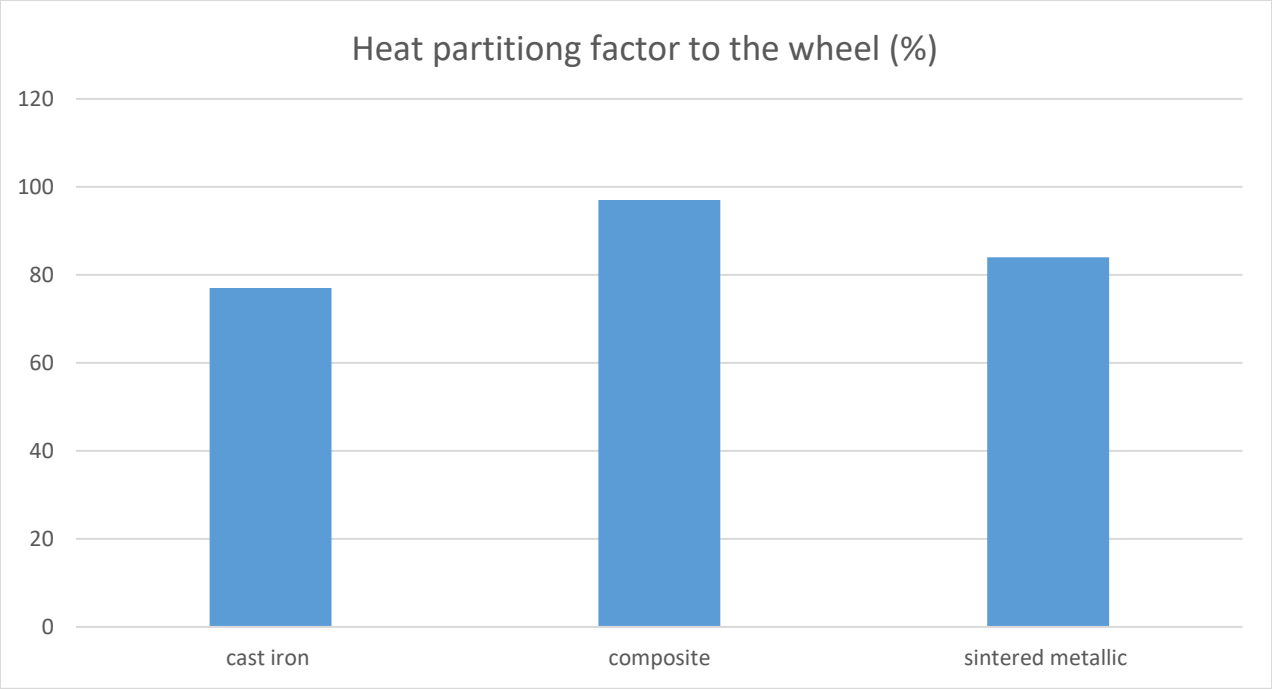

Figure 5-1:Comparison of the experimental heat partition factor for different brake-block materials.[17]

Figure 5-1 indicates a comparison of the heat partition factor α, as the fraction of frictional heat transferred to the wheel, for three different alternative brake block materials. The results indicate that composite blocks transfer the largest fraction of heat to the wheel, while cast iron exhibits a more moderate distribution, and sintered metallic blocks show intermediate behavior. [17] [18]

Additionally, literature shows that the 1Bg configuration produces higher temperature peaks on the tread, while the 2Bg configuration results in lower but more frequent temperature peaks. The 1Bg and 2Bg configurations referred to specific arrangements of brake systems that affect heat distribution. These differences also affect the heat diffusion in the wheel, changing thermal penetration depth and the overall temperature evolution during braking.

Finally, validating the numerical models with experimental investigations is an essential step. Comparing the simulation results with data from tests like twin-disc tribometer tests, scaled rig tests, or full-scale braking measurements helps researchers and engineers confirm that the model is correct. This assessment can be used to design safe and thermally efficient braking components for future railway applications.

6 Conclusion

The numerical simulation carried out for both 2D and 3D simulations, under steady-state and transient conditions, provides a complete assessment of the thermal behavior in tread-braked wheels. The 2D axisymmetric models, despite their simple geometry, successfully offered a reliable baseline for the average temperature evolution. However, the 3D model showed the influence of localized contact conditions on the thermal field.

The 3D model, including the brake block, showed the most realistic picture of the braking process. It had a non-uniform temperature distribution and much higher peak temperatures than the 2D and 3D models with uniform thermal load. The thermal concentration observed in this configuration is exactly consistent with the physical nature of tread braking, where frictional power is generated over a limited contact area, leading to localized heat accumulation.

The thermal analysis and obtained results emphasize the strong connection between the temperature field and wear behavior. Elevated temperatures accelerate the oxidation process, reduce material hardness through microstructural transformations, and promote crack initiation and propagation. These thermal damages lead to uneven wear and reduce wheel service life.

The thermal results from the simulations show how important it is to choose the right materials for both the wheel and the brake block. It is observed that any variations in thermal conductivity, specific heat capacity, hardness, and resistance to high-temperature degradation can directly influence the heat partitioning factor, temperature evolution and finally affect wear mechanisms during braking. Overall, the study confirms that accurate thermal modeling is a useful approach for wear prediction, supporting material optimization and improving the durability and reliability of tread-braked rail wheel systems.

7 References

1. N. Bosso, L. Cantone, G. Falcitelli, R. Gjini, M. Magelli, F. M. Nigro, E. Ossola, N. Zampieri, "Simulation of the thermo-mechanical behaviour of tread braked railway wheels by means of a 2D finite element model," *Tribology International*, vol. 178, 108074, 2023.
2. T. Vernersson, "Temperatures at railway tread braking. Part 1: Modelling," *Proceedings of the Institution of Mechanical Engineers, Part F: Journal of Rail and Rapid Transit*, vol. 221, no. 2, 167–182, 2007.
3. T. Vernersson, "Temperatures at railway tread braking. Part 2: Calibration and numerical examples," *Proceedings of the Institution of Mechanical Engineers, Part F: Journal of Rail and Rapid Transit*, vol., pp. 429–441, 2007.
4. M. Magelli, R. Pagano, N. Zampieri, "Adapting a scaled twin-disc device for tread braking investigations based on an ad-hoc thermal similitude model," *Wear*, manuscript WEA-S-25-00252, submitted, 2025.
5. M. Magelli, N. Zampieri, "A novel finite element axisymmetric model with non-axisymmetric thermal loads for thermal analyses of tread braked wheels," *Tribology International*, manuscript TRIBINT-S-25-00310, submitted, 2025.
6. R. Pagano, M. Magelli, N. Zampieri, "Design of an innovative twin-disc device for the evaluation of wheel and rail profile wear," *Designs*, vol. 8, no. 4, 73, 2024.
7. R. Pagano, *Innovative design of a Twin Disc tribometer for wheel-rail contact analysis*, MSc Thesis, Politecnico di Torino, Turin, Italy, A.Y. 2023/2024.
8. M. Magelli, N. Zampieri, Q. Wu, "Integration of brake block thermal equations within a railway vehicle multibody model: a multiphysics approach," *International Journal of Rail Transportation*, pp. 1–16, 2024.
9. A. Ekberg, E. Kabo,"Fatigue of railway wheels and rails under rolling contact and thermal loading – an overview,"
   Wear, vol. 258, no. 7–8, pp. 1288–1300, 2005.
10. A. Ekberg, B. Åkesson, Wheel/Rail Rolling Contact Fatigue – Analysis, Modelling and Practical Applications, Elsevier, Oxford, UK, 2014.
11. C. Kral, T. Vernersson,"Thermal loading of railway wheels due to tread braking,"
    Wear, vol. 258, no. 7–8, pp. 1317–1324, 2005.
12. M. Chiello, M. Firrone, P. Zucca,"Thermo-mechanical simulation of railway wheel braking and its influence on residual stresses,"
    Proceedings of the Institution of Mechanical Engineers, Part F: Journal of Rail and Rapid Transit, 2013.
13. S. Teimourimanesh, T. Vernersson, R. Lundén,
    "Braking capacity of railway wheels – State-of-the-art survey, "Proceedings of the 16th International Wheelset Congress (IWC16), March 2010
14. B. Karlsson, T. Vernersson,"Thermal contact conditions between brake block and wheel during railway tread braking,"
    Wear, vol. 314, pp. 28–37, 2014.

15. S. L. Grassie,“Rolling contact fatigue on the railway: a review,”
Wear, vol. 258, no. 7–8, pp. 1224–1236, 2005.
16. J. W. Ringsberg,“Life prediction of rolling contact fatigue crack initiation,”
International Journal of Fatigue, vol. 23, no. 7, pp. 575–586, 2001.
17. Y. Wang, Z. Jin, W. Zhang,“Numerical investigation of frictional heat generation and temperature evolution in railway braking,”
Applied Thermal Engineering, vol. 78, pp. 211–220, 2015.
18. R. Wasilewski, “Frictional heating and temperature distribution in braking systems – a review,” *Archives of Computational Methods in Engineering*, vol. 26, pp. 1123–1149, 2019.
19. Somà, L. D’Ambrosio, “Thermal analysis of railway wheels under tread braking using a 3D finite element model,” *Applied Sciences*, vol. 11, no. 11, 5010, 2021.
20. J. R. Barber, “Thermal contact problems,” *International Journal of Heat and Mass Transfer*, vol. 10, no. 10, pp. 1343–1350, 1967.
21. H. Blok, “The flash temperature concept,” *Wear*, vol. 6, pp. 483–494, 1963.
22. J. C. Jaeger, “Moving sources of heat and the temperature at sliding contacts,” *Proceedings of the Royal Society of New South Wales*, vol. 76, pp. 203–224, 1942.
23. F. E. Kennedy Jr., “Frictional heating and contact temperatures,” in *Modern Tribology Handbook*, B. Bhushan, Ed., CRC Press, Boca Raton, FL, USA, 2001.
24. D. Fletcher, S. Kapoor, “Thermal cracking in railway wheels,” *Wear*, vol. 258, no. 7–8, pp. 1149–1160, 2005.
25. M. F. Ashby, *Materials Selection in Mechanical Design*, 5th ed., Butterworth-Heinemann, Oxford, UK, 2017.
26. P. J. Blau, “Compositions, functions, and testing of friction brake materials and their additives,” Oak Ridge National Laboratory Report ORNL/TM-2001/64, Oak Ridge, TN, USA, 2001.
27. S. Eriksson, M. Bergman, S. Jacobson, “On the nature of tribological contact in automotive brakes,” *Wear*, vol. 252, no. 1–2, pp. 26–36, 2002.
28. S. H. Cho, K. J. Kim, “Thermal performance of brake friction materials: a review,” *International Journal of Automotive Technology*, vol. 12, no. 3, pp. 415–426, 2011.
29. S. Teimourimanesh, T. Vernersson, R. Lundén, “Braking capacity of railway wheels – State-of-the-art survey,” *Proceedings of the 16th International Wheelset Congress (IWC16)*, March 2010.